Electronic Supplementary Material (ESI) for RSC Advances.

Supporting Information

Zn^{2+} mediated solvent free solid state red emitting fluorescent complex formation in mortar-pestle along with living cell imaging studies

Susanta Adhikari [a]* Avijit Ghosh [a], Sandip Mandal [b], Animesh Sahana [b] and Debasis Das [b]

[a]*Department of Chemistry, University of Calcutta, 92, A.P.C. Road, Kolkata 700 009, West Bengal, India.*

[b]*Department of Chemistry, The University of Burdwan, Burdwan 713104, West Bengal, India.*

**Corresponding author. Department of Chemistry, University of Calcutta, 92, A.P.C. Road, Kolkata 700 009, West Bengal, India. Tel.: +91 33 23509937; fax: +91 33 23519755.*

E-mail address :adhikarisusanta@yahoo.com

General information

Chemicals and solvents were purchased from commercial suppliers and used as received. ^{1}H and ^{13}C NMR spectra were recorded on a Bruker Avance III HD (300 MHz) and an Avance III 500 (500 MHz) spectrometer. Chemical shifts were reported in parts per million (ppm), and the residual solvent peak was used as an internal reference: proton (chloroform δ 7.26), carbon (chloroform δ 77.16) or tetramethylsilane (TMS δ 0.00) was used as a reference. Multiplicity was indicated as follows: s (singlet), d (doublet), t (triplet), q (quartet), m (multiplet), dd (doublet of doublet), bs (broad singlet). Coupling constants were reported in Hertz (Hz). For thin layer chromatography (TLC), Merck precoated TLC plates (Merck 60 F254) were used, and compounds were visualized with a UV light at 254 nm.

Further visualization was achieved by staining with iodine. Flash chromatography separations were performed on SRL 230-400 mesh silica gel.

Synthesis of 2-(2-aminophenylamino) benzoic acid (**1**)

A mixture of 1, 2-phenylenediamine (2 gm, 18.50 mmol), 2-chloro benzoic acid (2.89 gm, 13.08 mmol), powdered Cu (200 mg), Cu_2O (200 mg), trans1, 2- cyclohexyldiamine (10 mol%) and K_2CO_3 (3.873gm, 27.75 mmol) in diglyme (30 mL) were heated under reflux for 8 h. Excess diglyme was removed by distillation and the mixture poured into 1L of hot water. Then 10 mL of 6(N) HCl was added to the mixture. The bluish black solid formed was filtered, washed and collected. The crude acid was dissolved in aqueous KOH, boiled in presence of activated charcoal and filtered. On acidification of the filtrate with HCl, a bluish black solid precipitate of **1** was obtained 1.26g (Yield ~30%). R_f: 0.41 (2 % methanol in dichloromethane); mp: 125-127 °C; ^{1}H NMR (Figure S5) (300 MHz, DMSO-d_6) δ 6.67 (m, 1H), 6.76 (m, 1H), 7.19 (d, 2H, J=7.2 Hz), 7.32 (d, 2H, J=7.2 Hz), 7.39 (d, 1H, J=6.9 Hz), 7.89 (d, 1H, J=6.6 Hz), 9.18 (s, 1H); HRMS (Figure S6) m/z $(M+H)^+$calcd for $C_{13}H_{12}N_2O_2N$: 229.2545 found: 229.0348.

Synthesis of 4-amino acridone (**2**)

400 mg (1.75 mmol) of **1** was taken in a round bottom flask to which 5 mL of Eaton's reagent was added. The mixture was heated under stirring condition in nitrogen atmosphere for 2 h, whereby the mixture turned to yellow colour. Then the reaction mixture was poured into 500 mL cold water and made alkaline by liquor ammonia. The greenish yellow precipitate formed was filtered, washed with water and dried. The crude solid was purified by silica gel column chromatography using 15% MeOH in dichloromethane as eluent to obtain **2** (238mg, yield ~65%) as light green solid.

R_f: 0.3 (10% methanol in dichloromethane); mp: 300°C; IR (neat) ν_{max} 3410.26, 1680.05, 1506.46, 1452.45, 1230.63, 1128.39; ^{1}H NMR (Figure S7) (300 MHz, DMSO-d_6) δ 6.90 (m, 2H), 7.10 (m, 1H), 7.40 (m, 1H), 7.60 (m, 2H), 8.11 (dd, 1H, J=8.25, 1.05 Hz), 10.522 (bs, 1H); HRMS (Figure S8) m/z $(M+H)^+$calculated for $C_{13}H_{10}N_2O$: 211.2393, found: 211.1820.

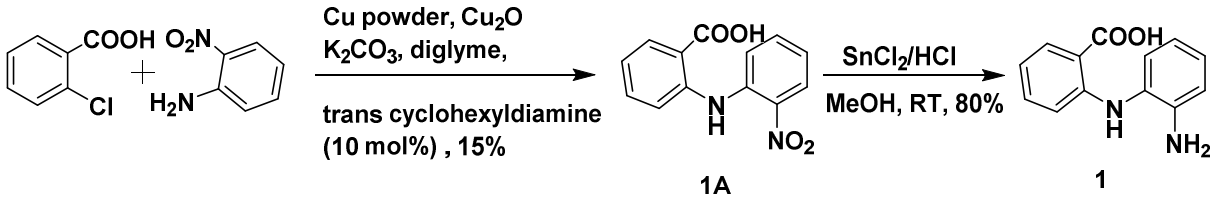

Scheme S1 Alternate synthetic route for **2-(2-aminophenylamino) benzoic acid** (**1**)

Synthesis of 2-((2-nitrophenyl) amino) benzoic acid (**1A**)

A mixture of *o*-nitro aniline (2 gm, 14.47 mmol), 2-chloro benzoic acid (2.25 gm, 13.08 mmol), powder Cu (200 mg), Cu_2O (200 mg), trans1, 2- cyclohexyldiamine (10 mol%) and K_2CO_3 (3.98 gm, 28.94 mmol) in diglyme (30 mL) were heated under reflux for 8 h. Excess diglyme was removed by distillation and the mixture poured into 1L of hot water. Then 10ml of 6(N) HCl was added to the mixture. The bluish black solid formed was filtered, washed and collected. The crude acid was dissolved in aqueous KOH, boiled in presence of activated charcoal and filtered. On acidification of the filtrate with HCl, a bluish black solid precipitate of 1A was obtained as crude which was purified by silica gel column chromatography using 1% Methanol in DCM to obtain pure **1A** (506mg, Yield ~15%) as yellow solid. R_f : 0.38 (3% methanol in DCM); mp: 137 °C; ^{1}H NMR (Figure S9) (300 MHz, DMSO-d_6) δ 7.31 (d, 1H, J=7.5 Hz), 7.44 (d, 1H, J=7.2 Hz), 7.60 (d, 1H, J=8.5 Hz), 8.11 (m, 4H), 8.41 (d, 1H, J=7.5 Hz); HRMS (Figure S10) m/z $(M+H)^+$ calculated. For $C_{13}H_{10}N_2O_4$: 259.0641, found: 259.0637.

Synthesis of 2-(2-aminophenylamino) benzoic acid (**1**)

A mixture of **1A** (500 mg, 1.93 mmol) and 1.74 mg of $SnCl_{2.}\ 2H_2O$ (7.72 mmol) are taken in 10 mL methanol and refluxed for 6 hours. After completion of the reaction as confirmed by TLC, methanol was evaporated in vacuum. The solid mass obtained was extracted with ethyl acetate, dried over Na_2SO_4 and purified by flash chromatography using 2% methanol in dichloromethane (352mg, Yield ~ 80%). R_f: 0.41 (2 % methanol in dichloromethane); mp: 125-127 °C; ^{1}H NMR (Figure S5) (300 MHz, DMSO-d_6) δ 6.67 (m, 1H), 6.76 (m, 1H), 7.19 (m, 2H), 7.32 (m, 2H), 7.39 (m, 1H), 7.89 (dd, 1H, J=7.95, 1.35 Hz), 9.18 (s, 1H); HRMS (Figure S6) m/z $(M+H)^+$ calcd. For $C_{13}H_{12}N_2O_2N$: 229.2545, found: 229.2543.

Preparation of AAS-Zn complex

100 mg (0.3181 mmol) of AAS was dissolved in 10 mL methanol. Then 95 mg (0.3193 mmol) of $Zn(NO_3)_{2.}\ 6H_2O$was added to the solution and stirred the mixture for 1 h. A deep red solid precipitated which was filtered, washed with cold methanol and dried in vacuum. The red solid was characterised by NMR. ^{1}H NMR (300 MHz, DMSO-d6) (Figure S33): δ 6.56 (m, 1H), 6.75 (m, 1H), 7.04 (m, 1H), 7.12 (m, 1H) 7.48 (m, 2H), 7.97 (m, 2H), 8.02 (m, 2H), 8.19 (m, 2H), 9.21 (s, 1H); HRMS (ESI) (Figure S35): m/z $(M + Na)^+$ calcd. for $C_{40}H_{26}N_4O_4Zn$: 713.113 found: 710.4402. IR (neat) ν_{max} 3057.17, 1600.91, 1498.69, 1438.89, 1394.53, 1251.80, 1153.43, 756.09 (Figure S36).

Preparation of AAS-Zn^{2+} complex under solvent free condition

25 mg (0.0795 mmol) of **AAS** was taken into a mortar and grinding with a pestle. After 3 minutes of grinding, 23.5 mg (0.0789 mmol) of $Zn(NO_3)_2.6H_2O$ was added to the same mortar and grinded for another 2 minutes. A deep yellowish-red solid was obtained, which gives a strong red fluorescence under UV-lamp.

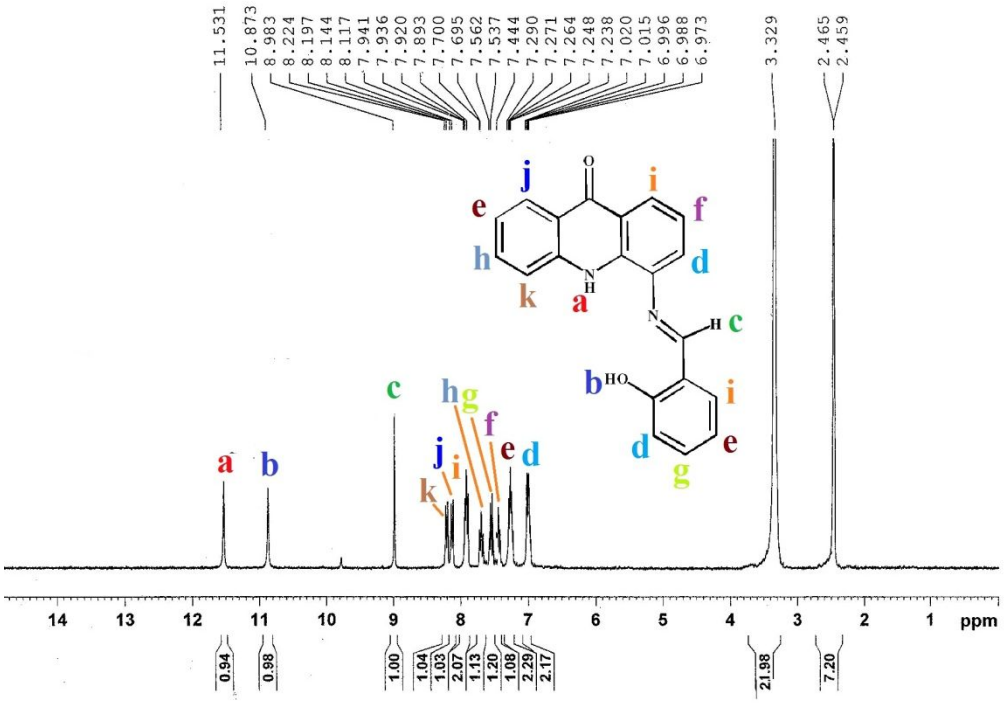

Figure S1 ^{1}H NMR spectrum of **AAS** in DMSO-d_6.

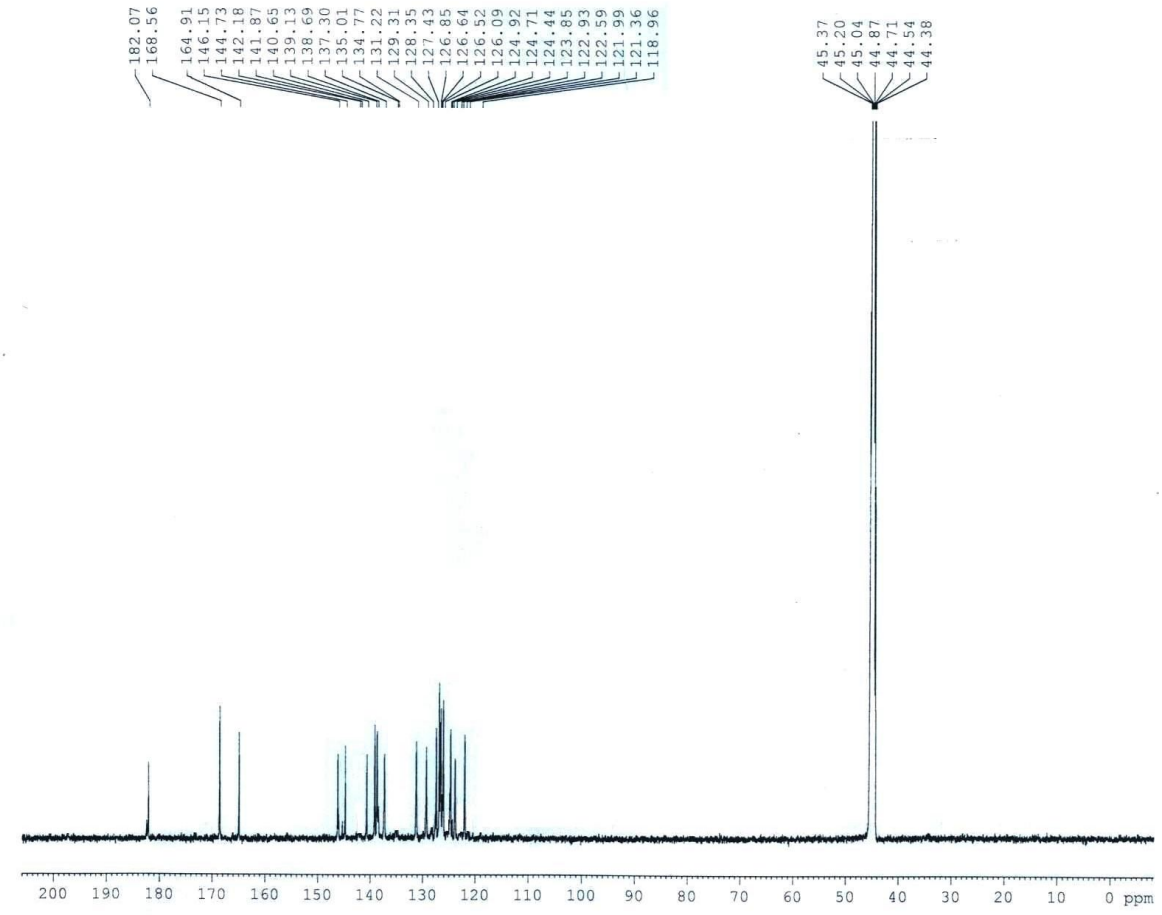

Figure S2 ^{13}C NMR spectrum of **AAS** in DMSO-d_6.

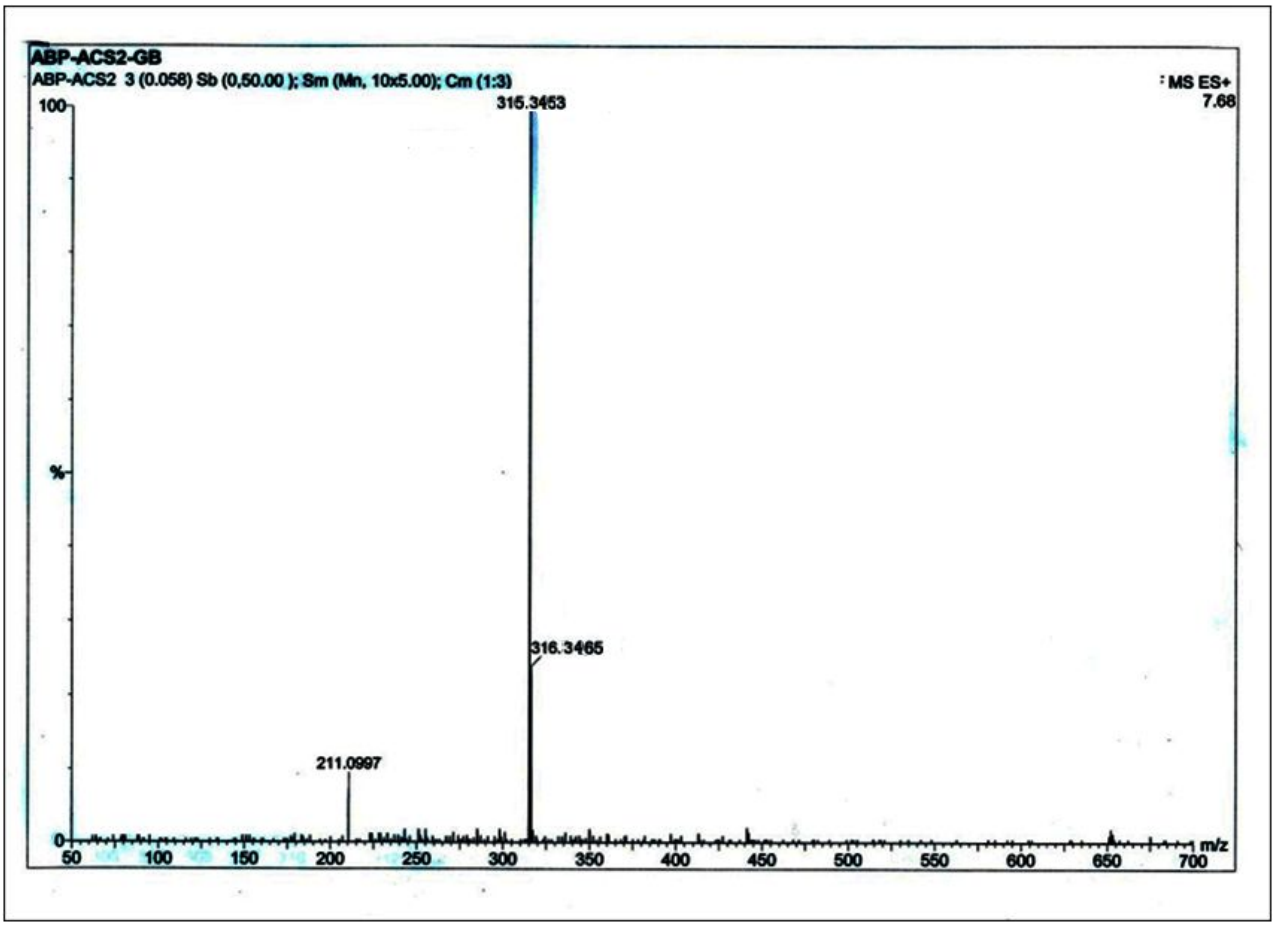

Figure S3 HRMS spectrum of **AAS.**

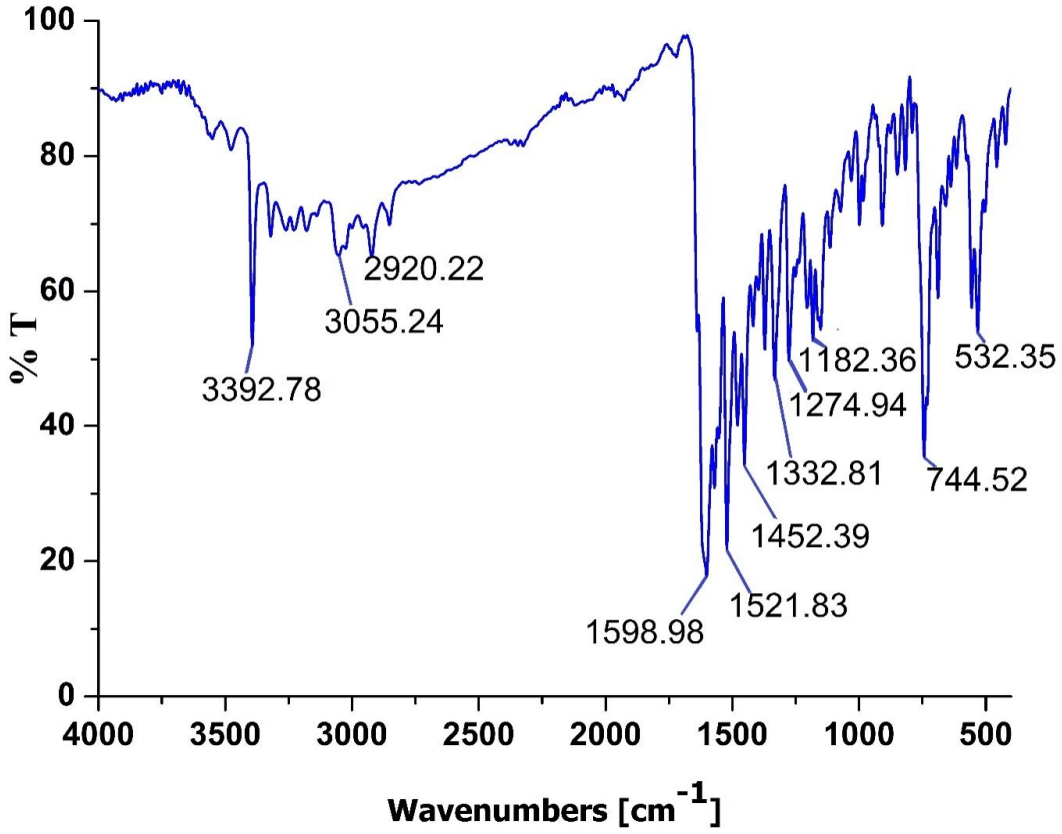

Figure S4 ATIR spectrum of **AAS.**

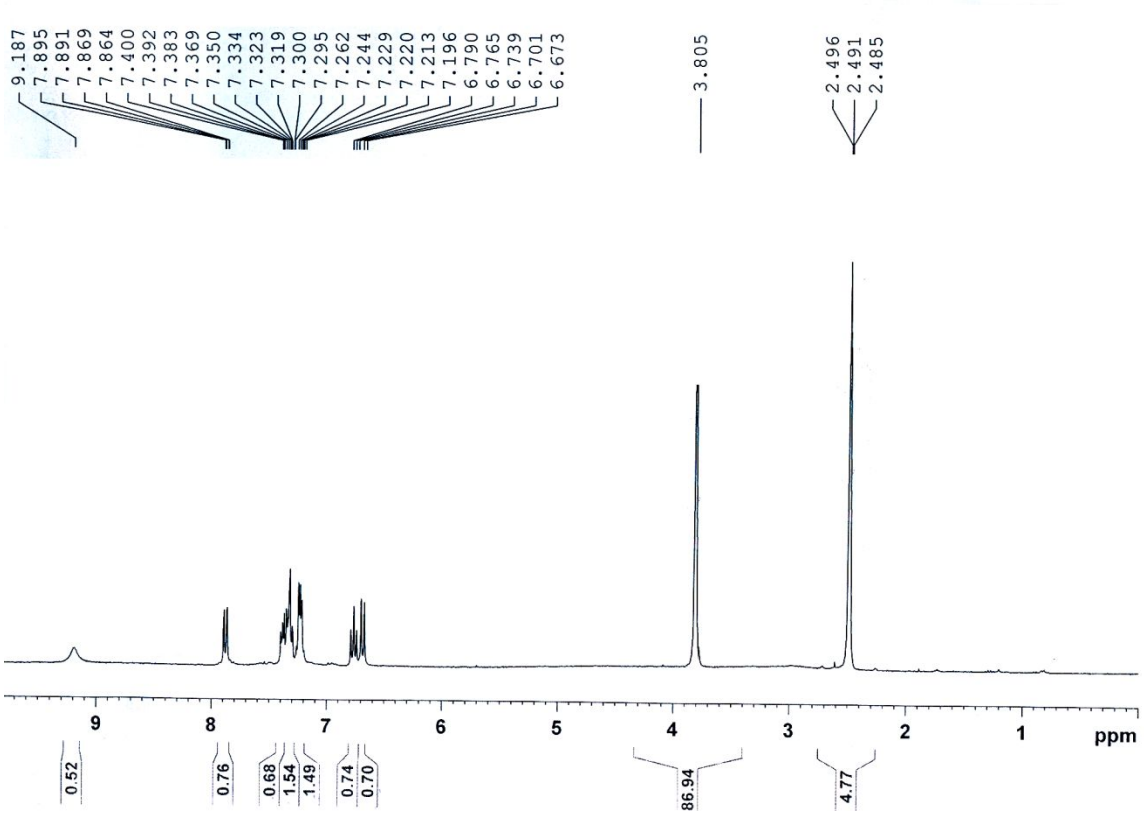

Figure S5 ^{1}H NMR spectrum of **2-(2-aminophenylamino) benzoic acid (1)** in DMSO-$d_{6.}$

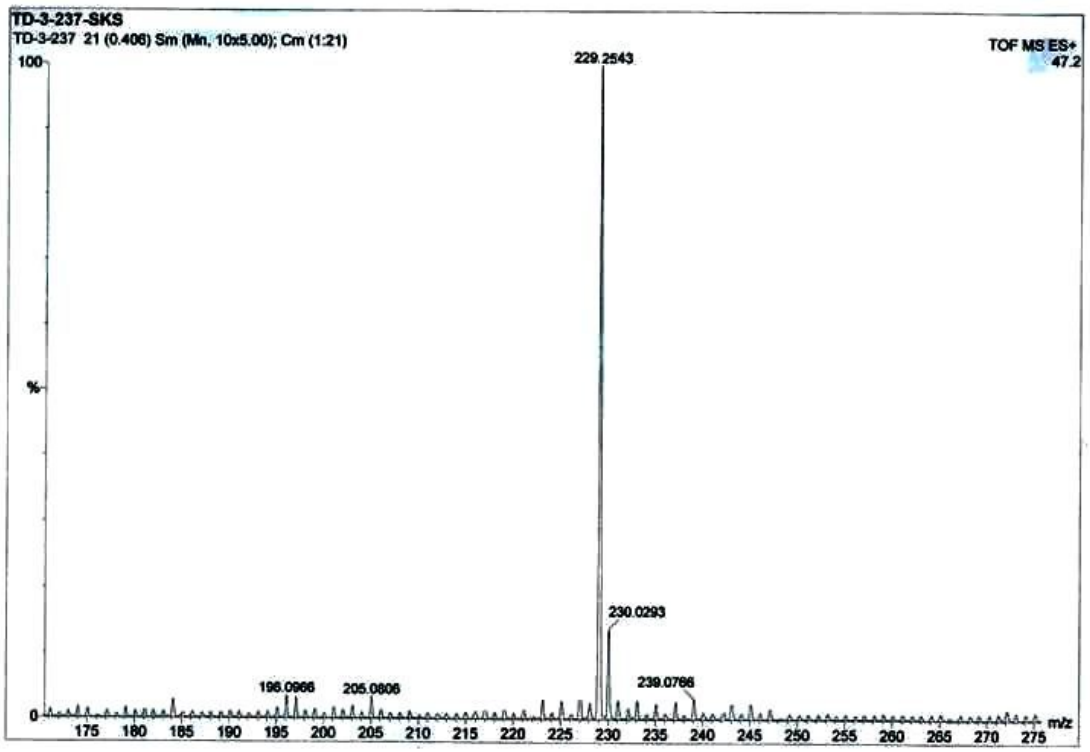

Figure S6 TOF MS of **2-(2-aminophenylamino) benzoic acid** (**1**) in methanol.

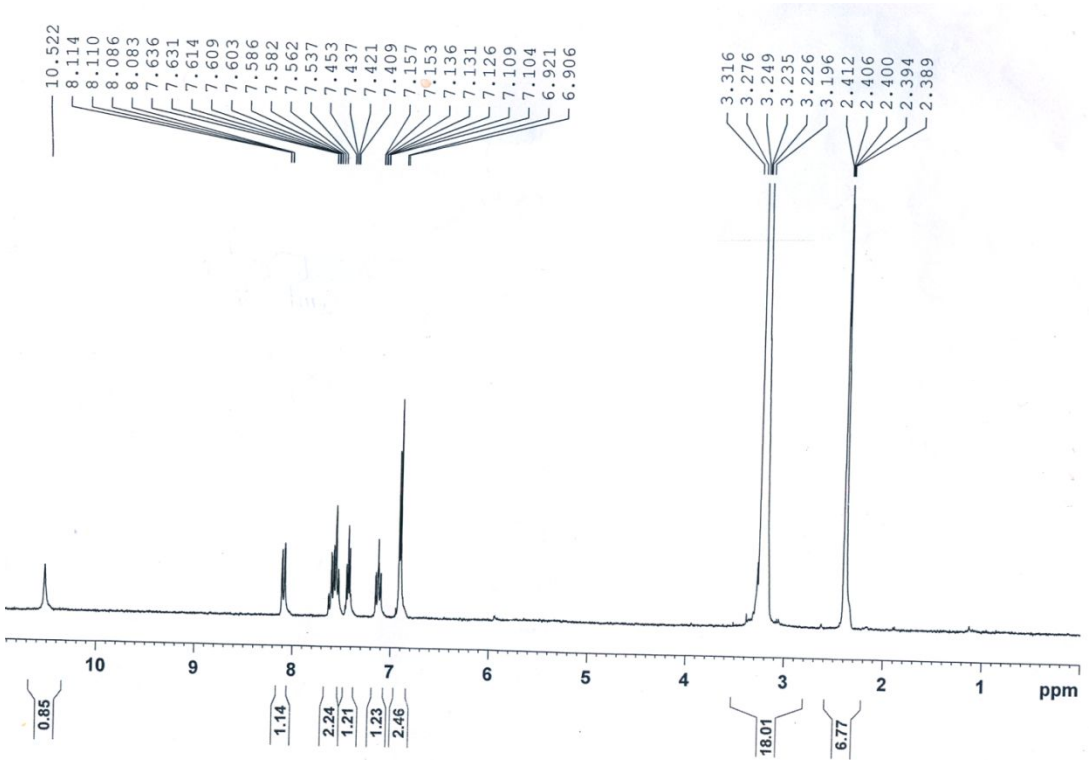

Figure S7 ^{1}H NMR spectrum of **4-amino acridone** (**2**) in DMSO-d_6.

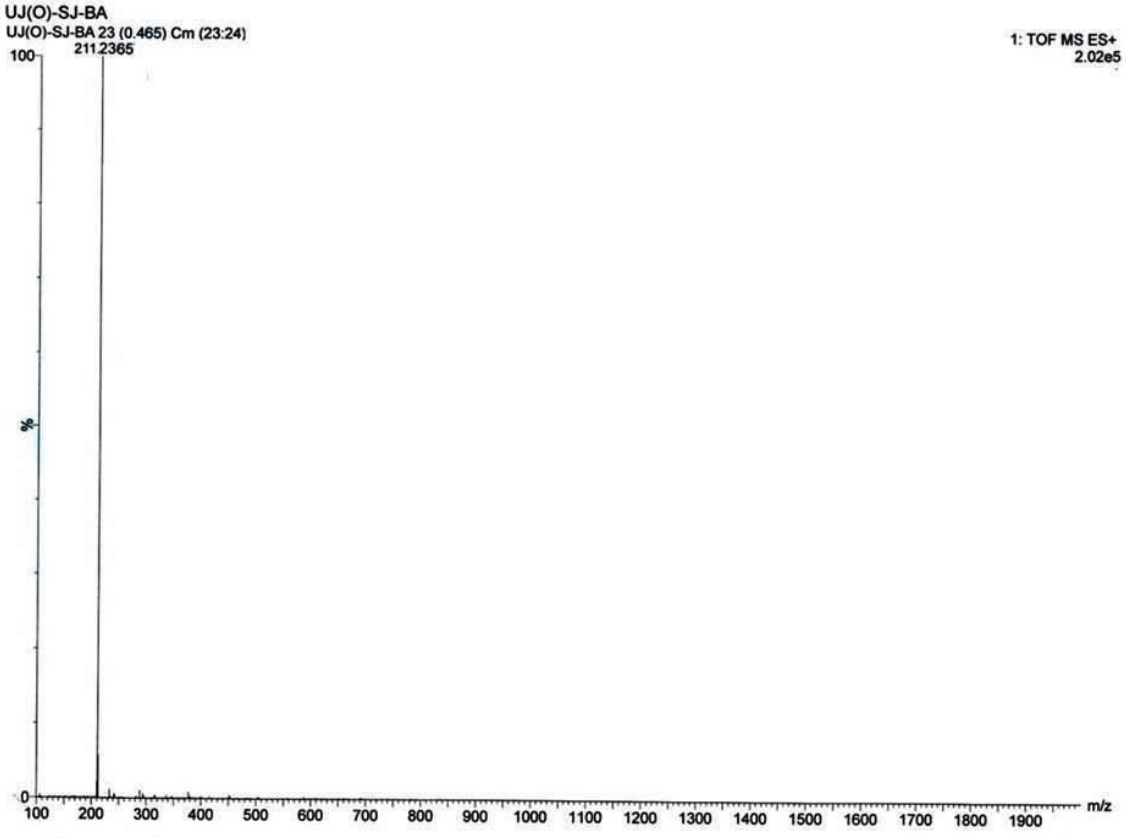

Figure S8 TOF MS spectrum of **4-amino acridone** (**2**) in methanol.

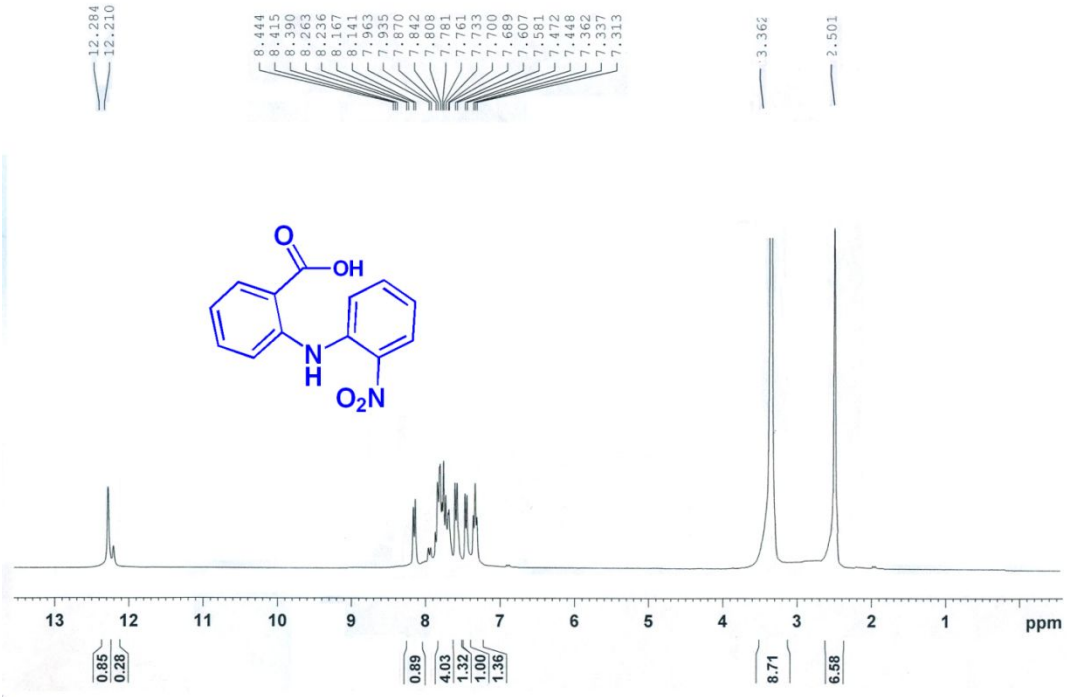

Figure S9 ^{1}H NMR spectrum of **2-((2-nitrophenyl) amino) benzoic acid (1A)** in DMSO-d_6.

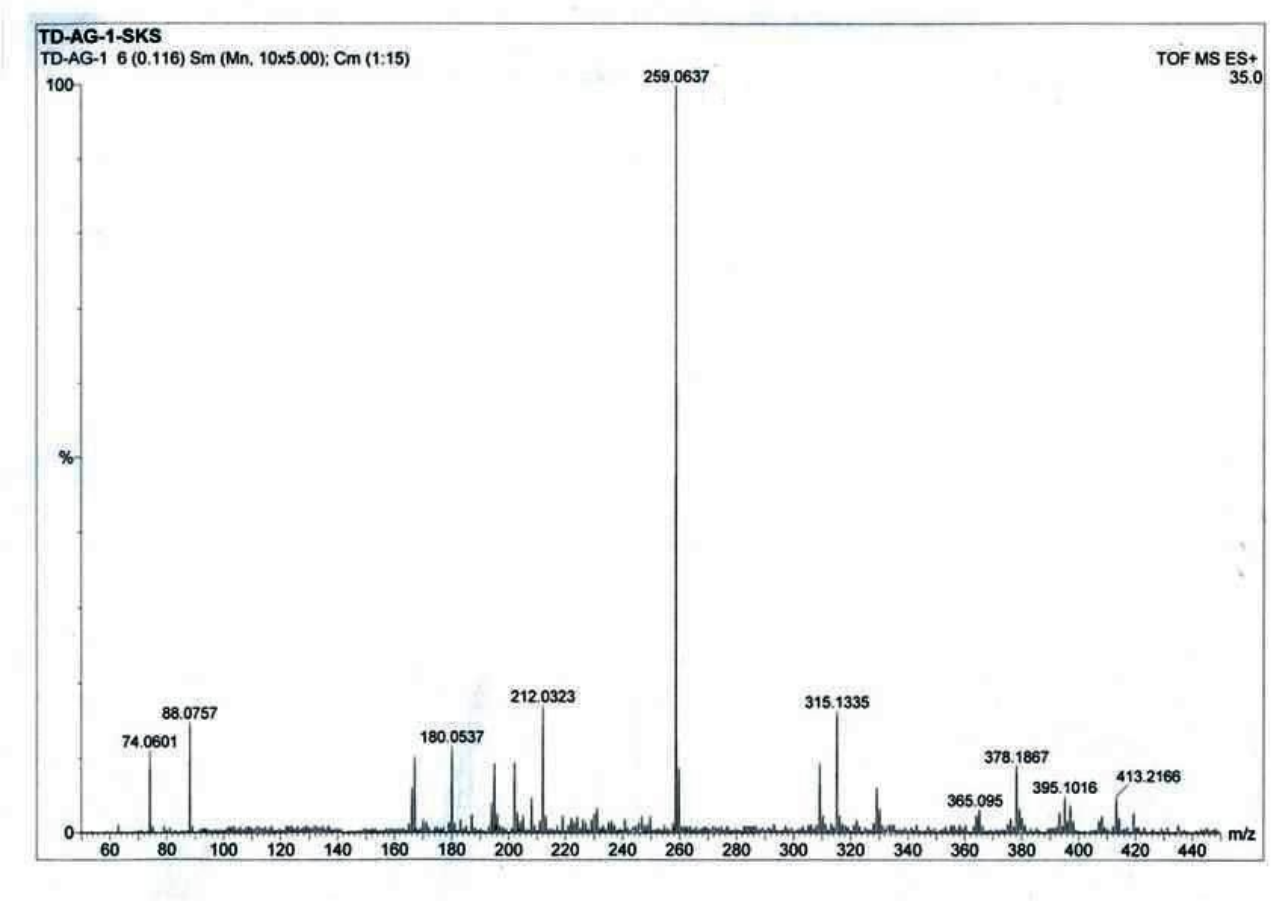

Figure S10 TOF MS spectrum of **2-((2-nitrophenyl) amino) benzoic acid (1A)** in methanol.

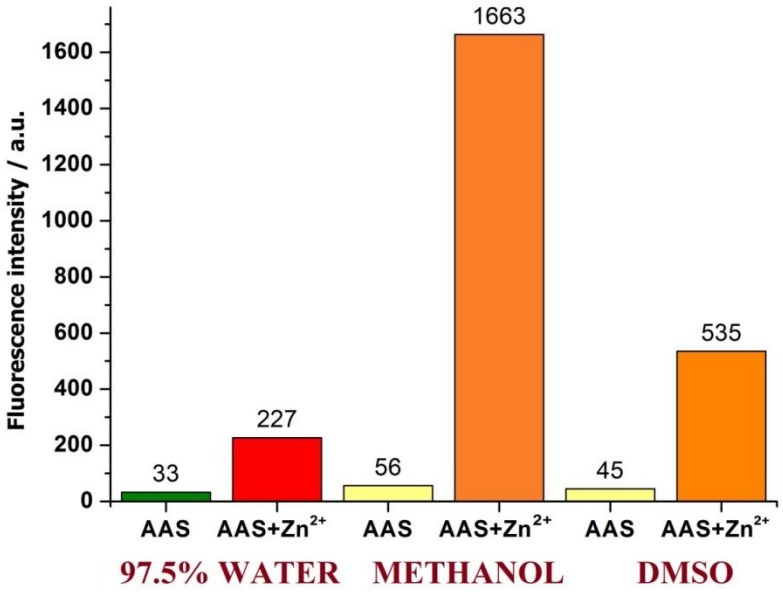

Figure S11 Emission profile (λ_{ex} = 445 nm) in different solvents: λ_{em}; 1. **AAS**→528 nm and **AAS+Zn**$^{2+}$ → 565 nm in 97.5: 2.5 (water: methanol, v/v); 2. **AAS** → 542 nm and **AAS+Zn**$^{2+}$ → 560 nm in dry methanol; 3. **AAS** → 545 nm and **AAS + Zn**$^{2+}$ → 560 nm in DMSO.

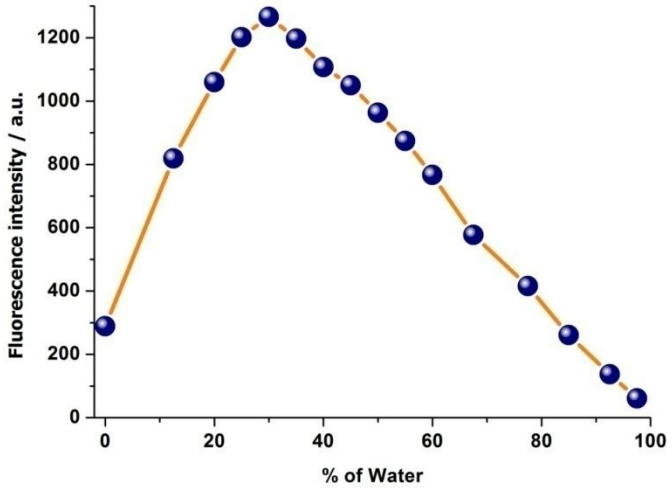

Figure S12 Changes of emission intensities of **AAS** (50 µM) with increasing water content (%, v/v) in dry methanol (λ_{ex} = 445 nm). Emission intensities are recorded at their corresponding λ_{em}, which changes from 542 nm in dry methanol to 528 nm in 97.5: 2.5 (water: methanol, v/v).

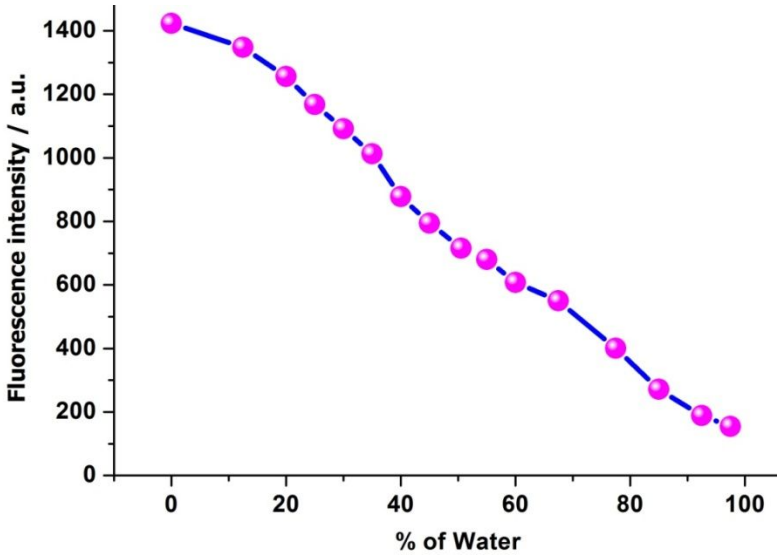

Figure S13 Changes of emission intensities of **AAS** (50 μM) in presence of Zn^{2+} (100 μM) with increasing water content (%, v/v). Emission intensities are recorded at their corresponding λ_{em}, which changes from 560 nm in dry methanol to 565 in 97.5: 2.5 (water: methanol, v/v).

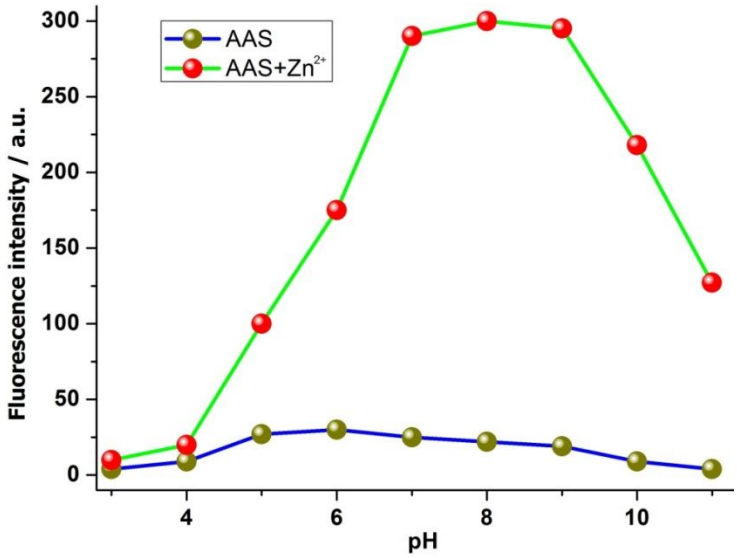

Figure S14 Effect of pH on the emission intensity of **AAS** (10 μM) and **[AAS–Zn^{2+}]** (50 μM) systems in water: methanol (97.5: 2.5, v/v).

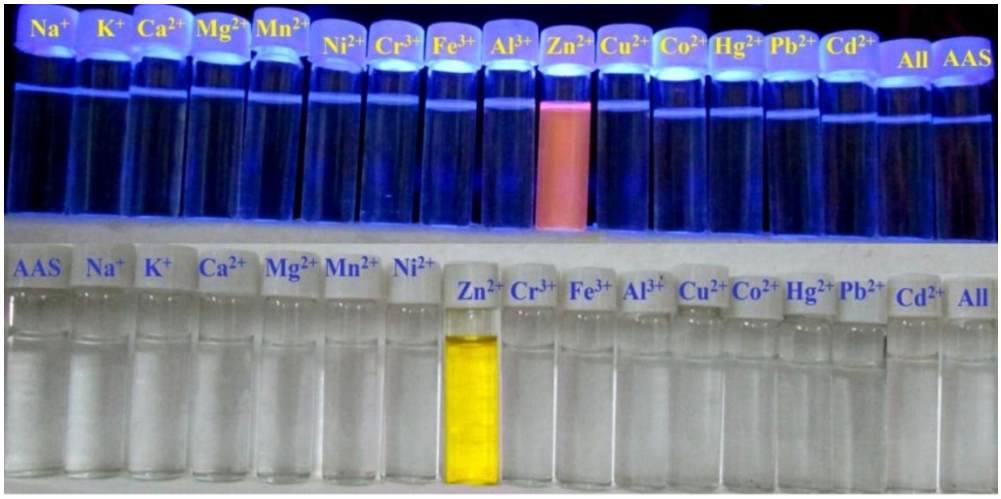

Figure S15 Emission colours of **AAS** (10 µM) in dry methanol in presence of common cations (Na^+, K^+, Ca^{2+}, Mg^{2+}, Mn^{2+}, Ni^{2+}, Cr^{3+}, Fe^{3+}, Al^{3+}, Zn^{2+}, Cu^{2+}, Co^{2+}, Hg^{2+}, Pb^{2+}, Cd^{2+}, All cations (100 µM) and free **AAS** under UV lamp (top) and through naked eye (bottom) .

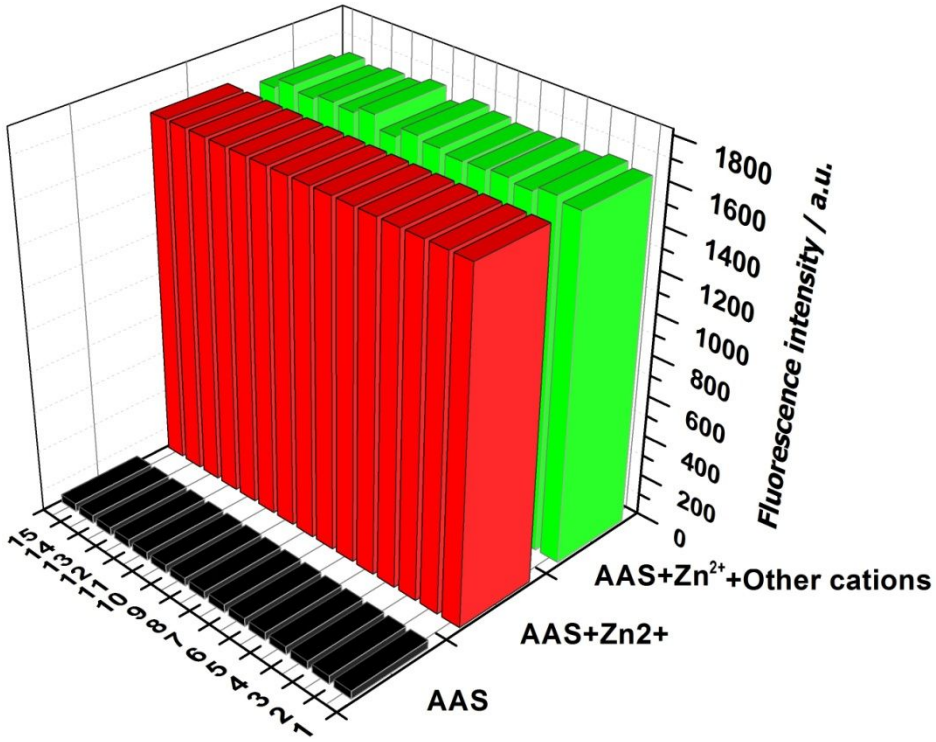

Figure S16 Plot of emission intensities of **AAS-Zn^{2+}** adduct in presence of different cations: [**AAS** (10 µM) + Zn^{2+} (100 µM)**].** Cations: 1. Na^+, 2. K^+, 3. Ca^{2+}, 4. Mg^{2+}, 5. Mn^{2+}, 6. Ni^{2+}, 7. Cr^{3+}, 8. Fe^{3+}, 9. Al^{3+}, 10. Cu^{2+}, 11. Co^{2+}, 12. Hg^{2+}, 13. Pb^{2+}, 14. Cd^{2+} and 15. all cations (100 µM) in dry methanol (λ_{ex} = 445 nm).

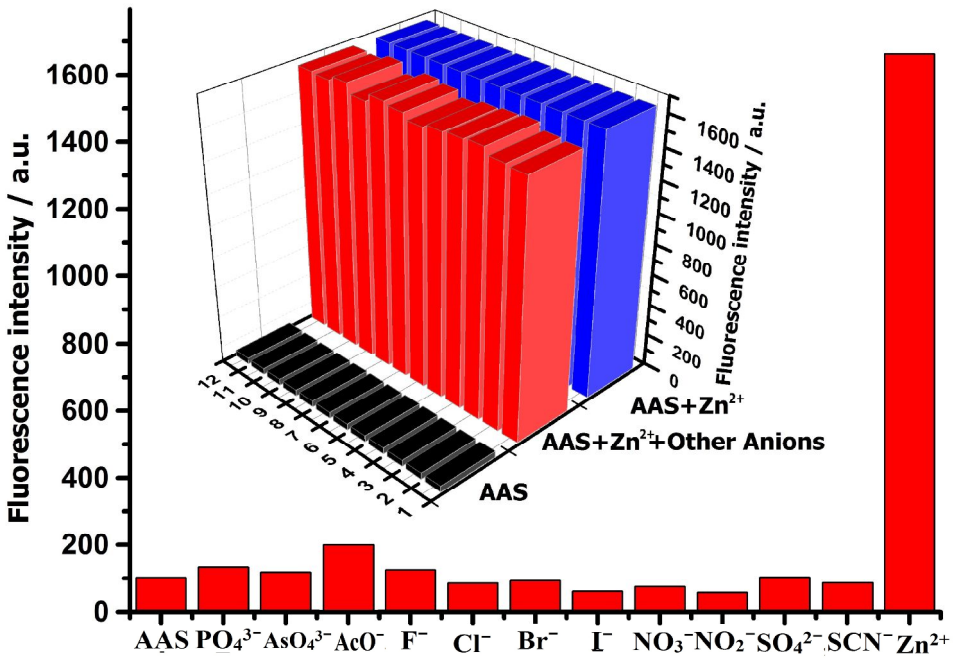

Figure S17 Fluorescence emission intensities of **AAS** (10 μM) in presence of common anions (100 μM) in dry methanol: 1. Free **AAS**, 2. PO_4^{3-}, 3. AsO_4^{3-}, 4. AcO^-, 5. F^-, 6. Cl^-, 7. Br^-, 8. I^-, 9. NO_3^-, 10. NO_2^-, 11. SO_4^{2-}, 12. SCN^- and 13. 100 μM Zn^{2+}; λ_{em} = 565 nm. Inset: represent the interferences of anions.

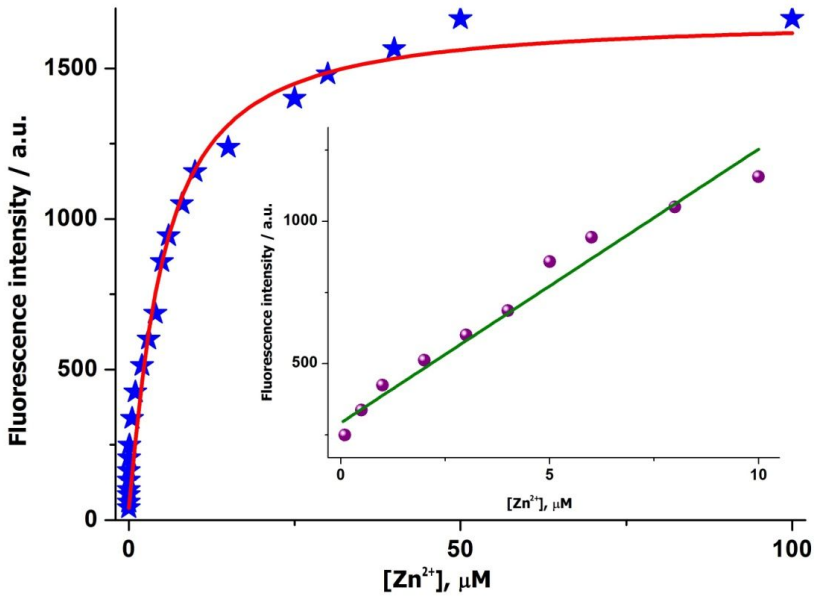

Figure S18 Plot of emission intensity of **AAS** (10 μM) as a function of externally added Zn^{2+}(0.0001–100 μM) in dry methanol. Inset: linear region (up to 10 μM Zn^{2+}).

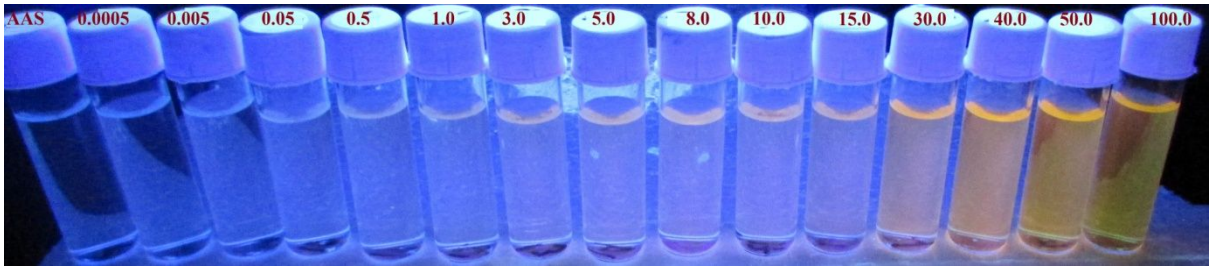

Figure S19 Colour changes of **AAS** (10 μM) upon gradual addition of Zn^{2+} (μM) in dry methanol under hand held UV lamp.

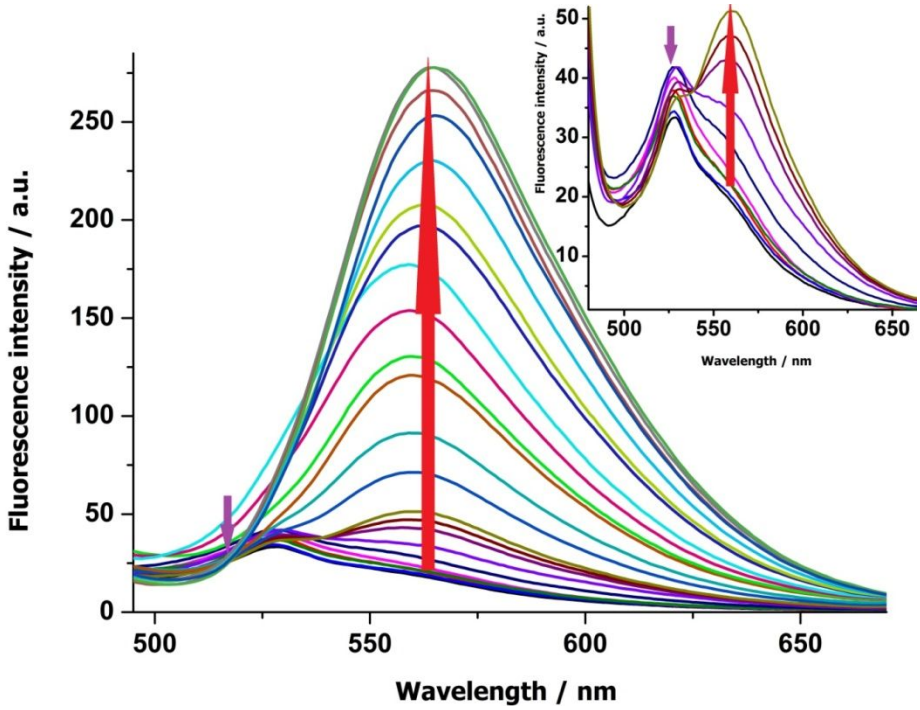

Figure S20 Changes in the fluorescence spectra of **AAS** in HEPES buffered (0.1 M, pH 7.4), water: methanol (97.5: 2.5, v/v), upon gradual addition of Zn^{2+} (0.0001, 0.0005, 0.001, 0.005, 0.01, 0.05, 0.1, 0.5, 1.0, 2.0, 3.0, 4.0, 5.0, 6.0, 8.0, 10.0, 15.0, 25.0, 30.0, 40.0, 50.0, and 100.0 μM). Inset: lower concentration spectra (0.0001 μM to 1.0 μM).

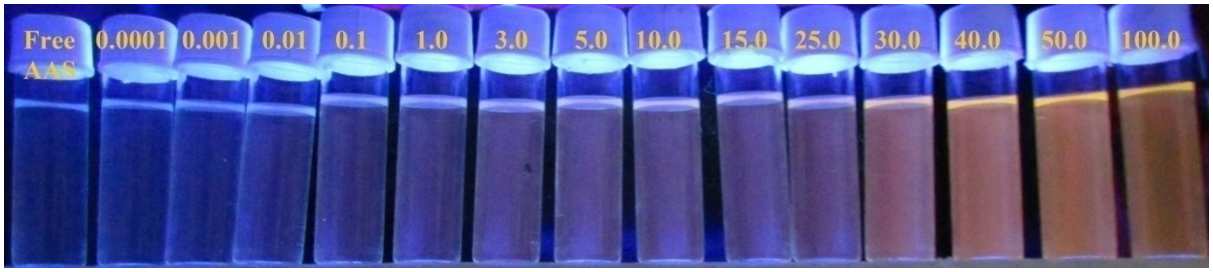

Figure S21 Colour changes of **AAS** (10 μM) in HEPES buffered (0.1 M, pH 7.4) water: methanol (97.5: 2.5) media upon gradual addition of Zn^{2+} (Free **AAS**, 0.0001, 0.001, 0.01, 0.1, 1.0, 3.0, 5.0, 10.0, 15.0, 25.0, 30.0, 40.0, 50.0, and 100.0 μM Zn^{2+}) under hand held UV lamp.

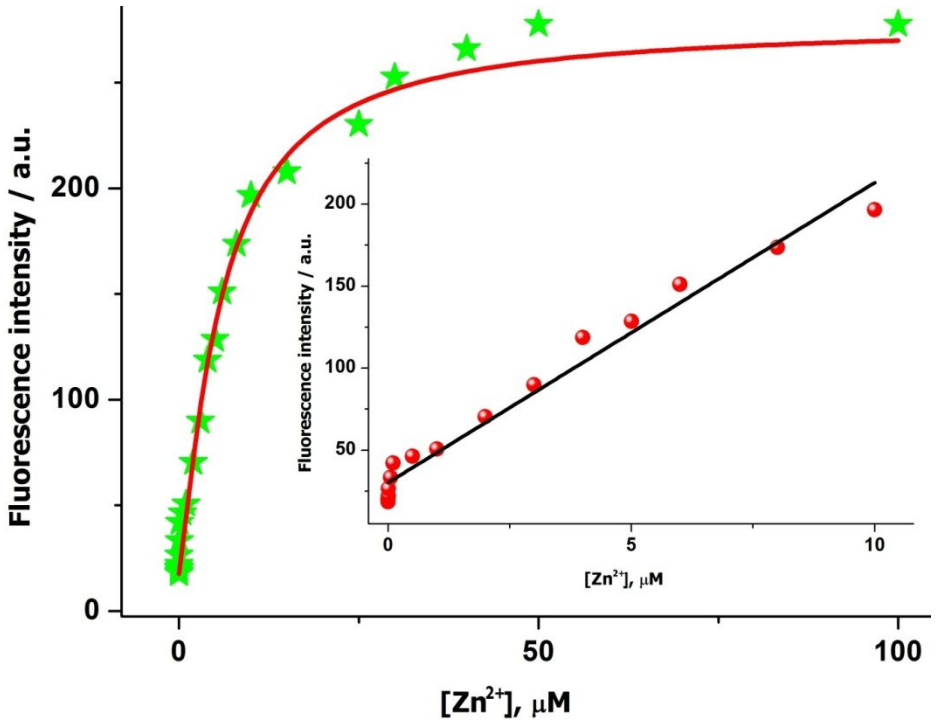

Figure S22 Plot of emission intensity of **AAS** (10 μM) as a function of externally added Zn^{2+}(0.0001–100 μM) in HEPES buffered (0.1 M, pH 7.4) water: methanol (97.5: 2.5, v/v). Inset shows the linear region up to 10 μM Zn^{2+}.

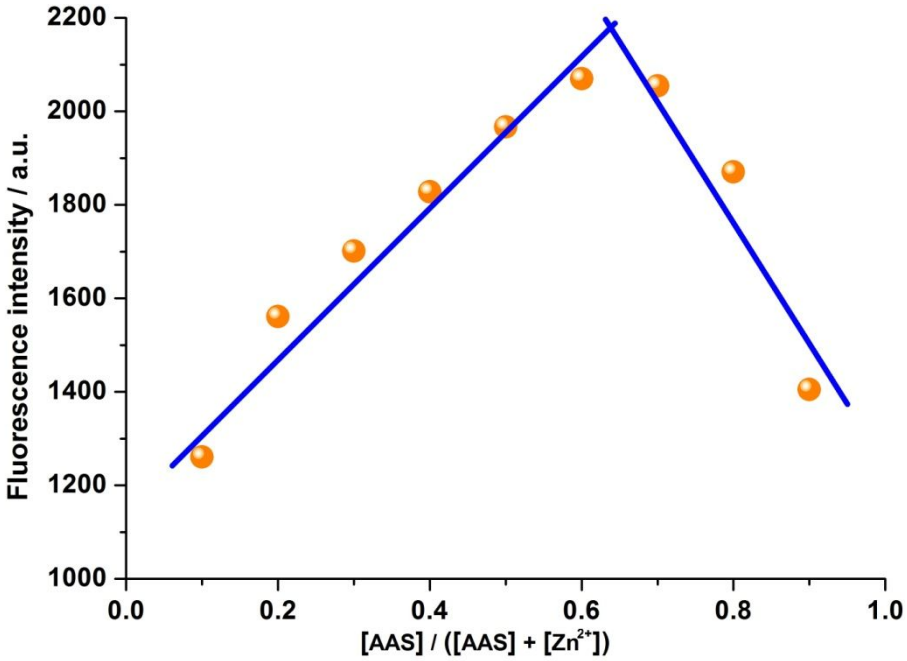

Figure S23 Job's plot (stoichiometry determination of the **AAS-Zn^{2+}** adduct) in dry methanol.

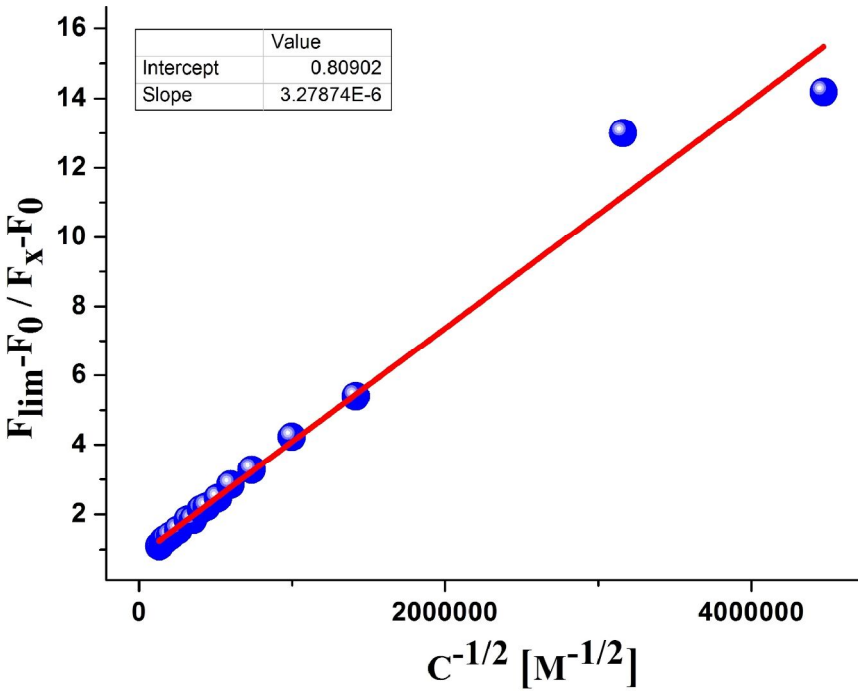

Figure S24 Determination of the equilibrium binding constant of **AAS** for **Zn^{2+}** (fluorescence technique).

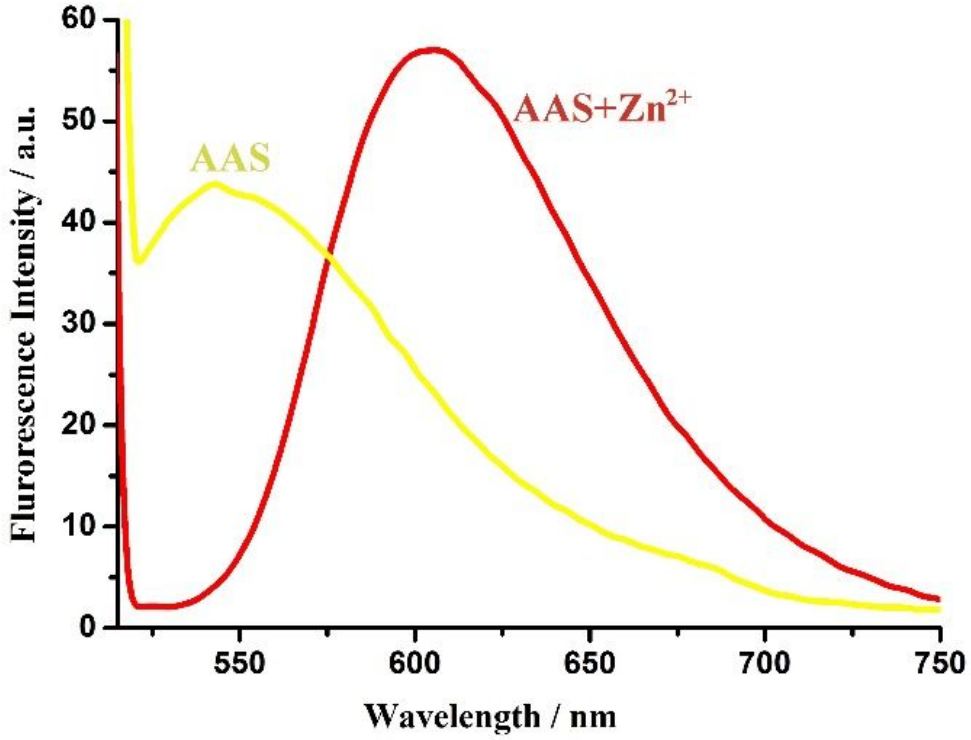

Figure 25 Solid state fluorescence spectra of **AAS** and **AAS+Zn^{2+}** adduct. Emission of **AAS** and **AAS+Zn^{2+}**adduct occur at 544 nm and 605 nm respectively ($\lambda_{ex,}$ 495 nm).

Figure S26 Naked eye colour of **AAS** (a) and **AAS+Zn^{2+}** adduct (b). (c) and (d) are respective colours under hand held UV lamp.

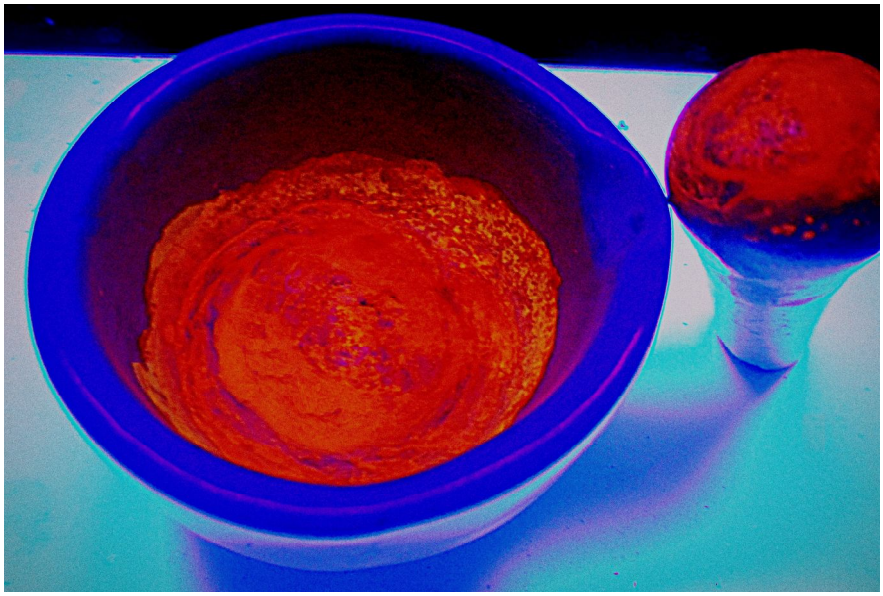

Figure S27 Naked eye colour of **AAS+Zn^{2+}** adduct in presence of common anions under hand held UV lamp.

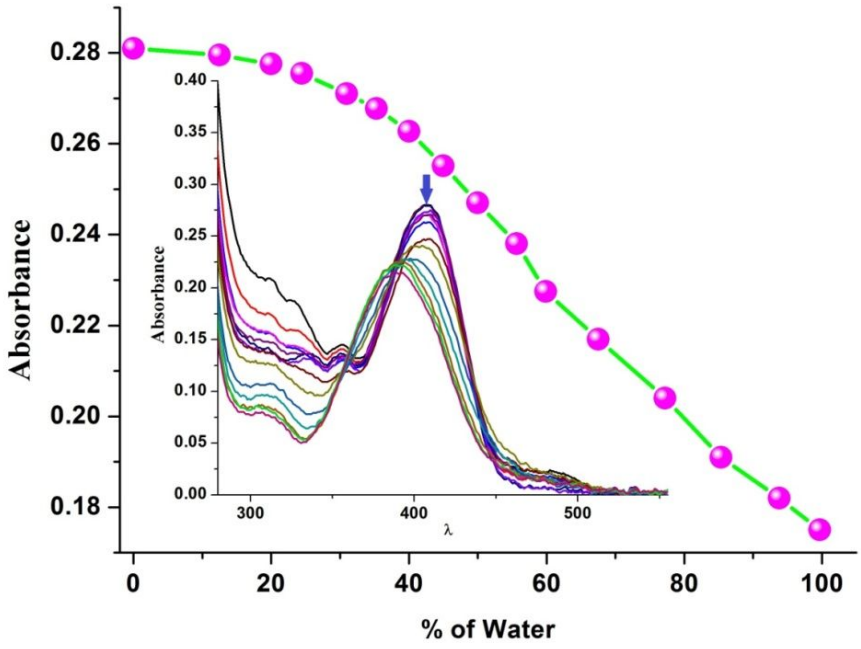

Figure S28 Changes of absorbance of **AAS** (50 µM) at 409 nm with increasing water (%, v/v) in methanol. Inset: changes in the absorption spectra of **AAS** as a function of added water.

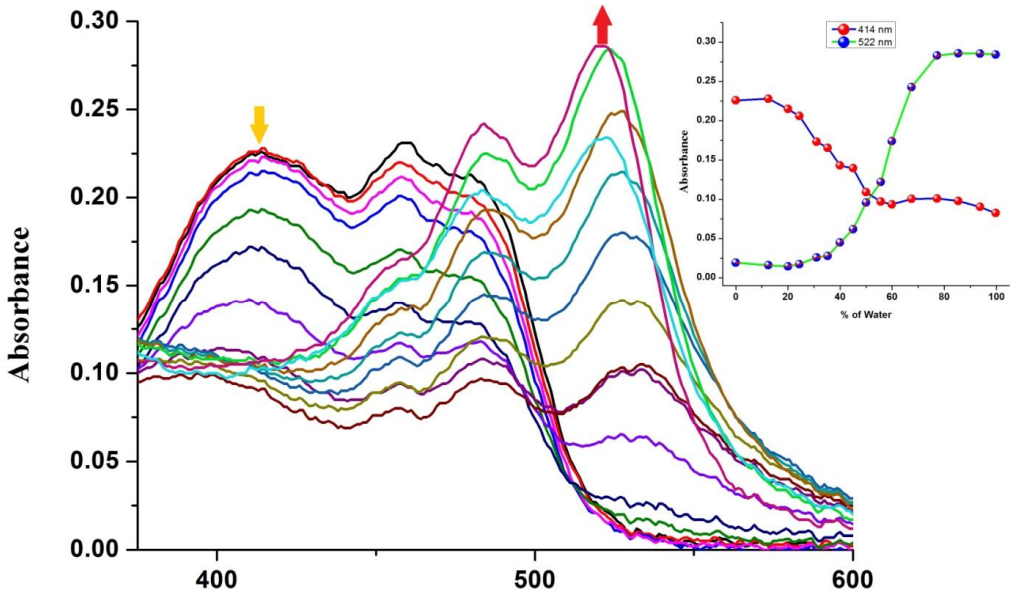

Figure S29 Change in absorbance of **AAS** (50 μM) in presence of **Zn^{2+}** (100 μM) at 414 nm and 522 nm with increasing amount of water (%, v/v) in methanol. Inset: plot of absorbance changes of **AAS-Zn^{2+}** system at two different wavelengths.

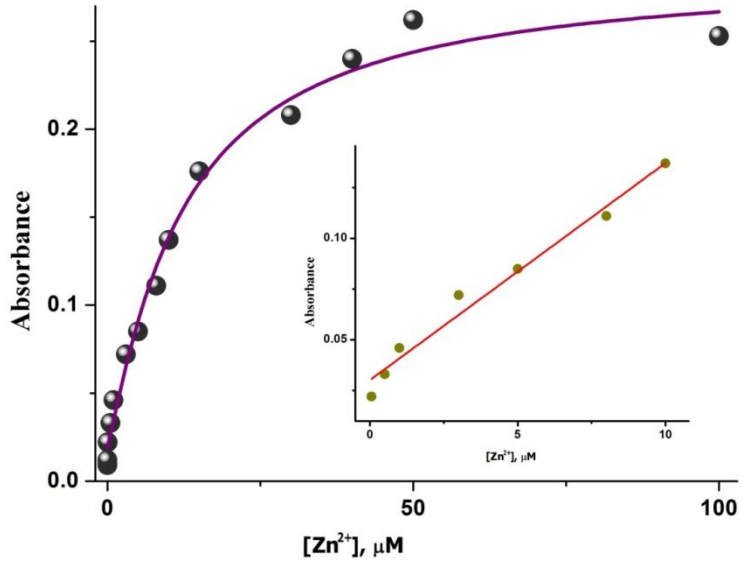

Figure S30 Plot of absorbance of **AAS** (10 μM, λ, 462 nm) as a function of added Zn^{2+}(0.0001–100 μM) in dry methanol Inset shows the linear region, up to 10 μM Zn^{2+}.

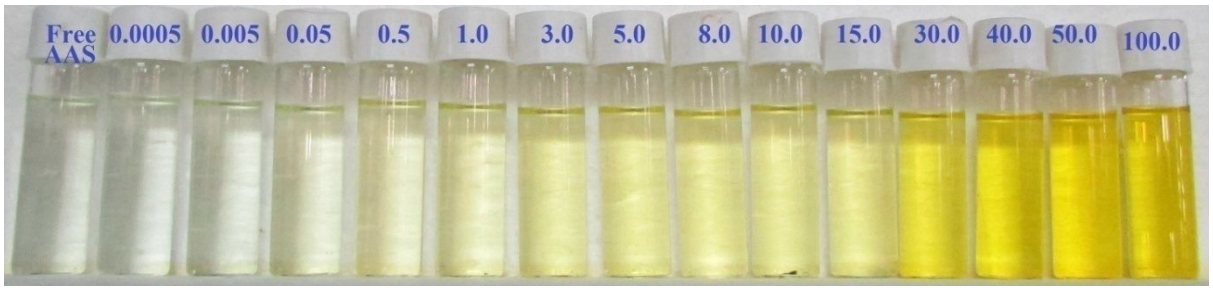

Figure S31 Naked eye colour of **AAS** (10 µM) in dry methanol upon gradual addition of Zn^{2+} (from left, free **AAS** followed by different amount of Zn^{2+} in µM).

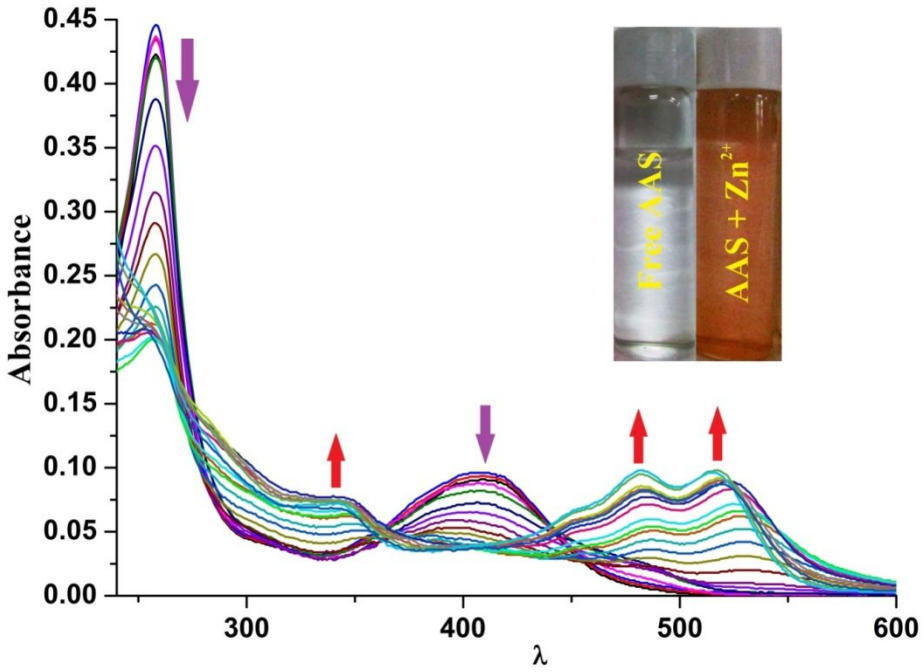

Figure S32 Absorbance of **AAS** (10 µM) in HEPES buffered (0.1 M, pH 7.4) aqueous methanol (water: methanol 97.5: 2.5, v/v) upon gradual addition of Zn^{2+} (Free **AAS**, 0.0001, 0.0005, 0.001, 0.005, 0.01, 0.05, 0.1, 0.5, 1.0, 2.0, 3.0, 4.0, 5.0, 6.0, 8.0, 10.0, 15.0, 25.0, 30.0, 40.0, 50.0, and 100.0 µM Zn^{2+}). Inset: Colour of free **AAS** and **AAS-Zn^{2+}** adduct.

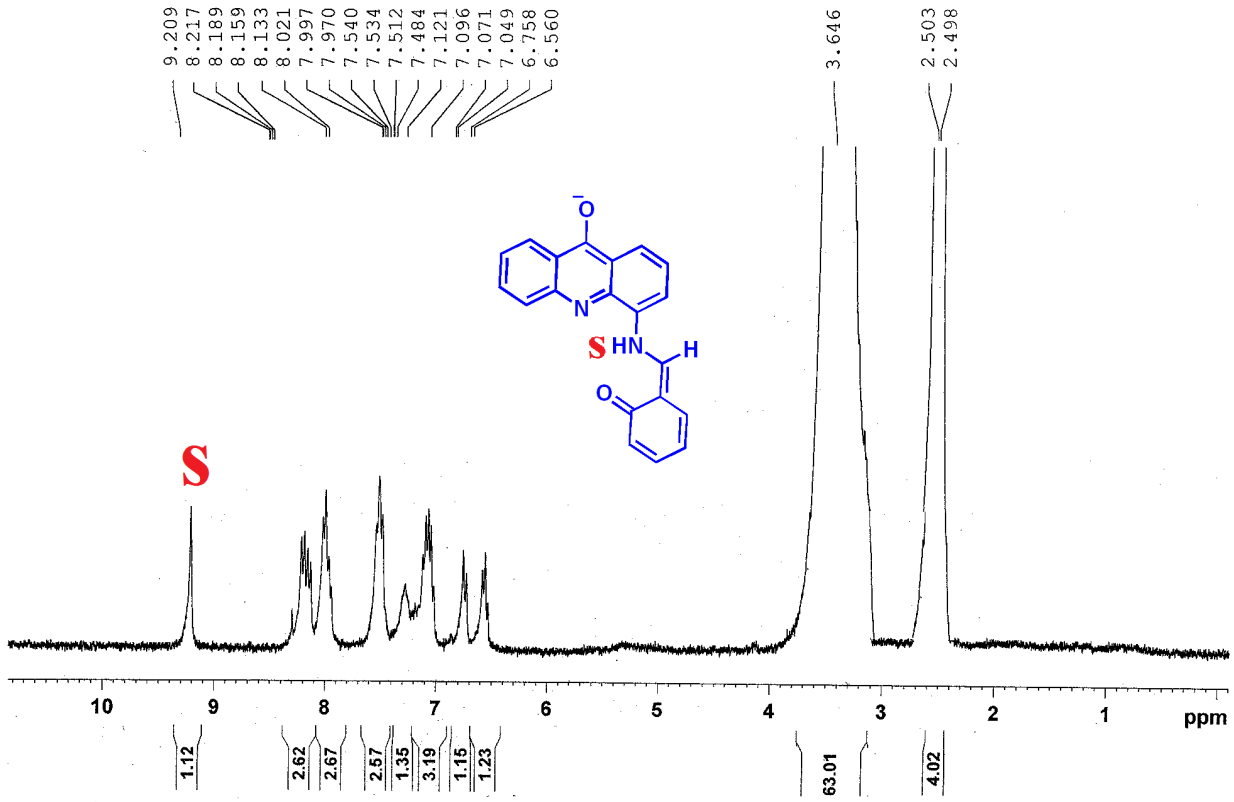

Figure S33 ^{1}H NMR spectrum of isolated red colour **AAS** +Zn^{2+} complex in DMSO-d_6 (very poor solubility).

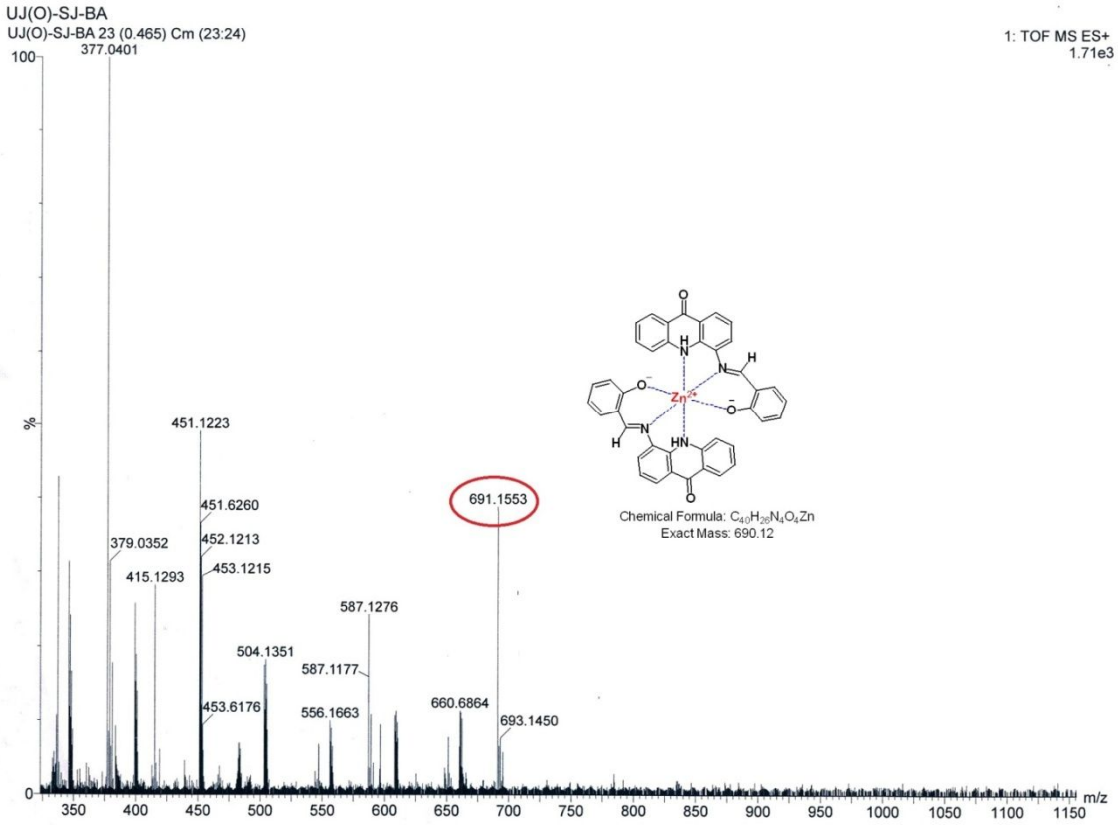

Figure S34 TOF MS spectrum of **AAS** and Zn^{2+} complex in methanol.

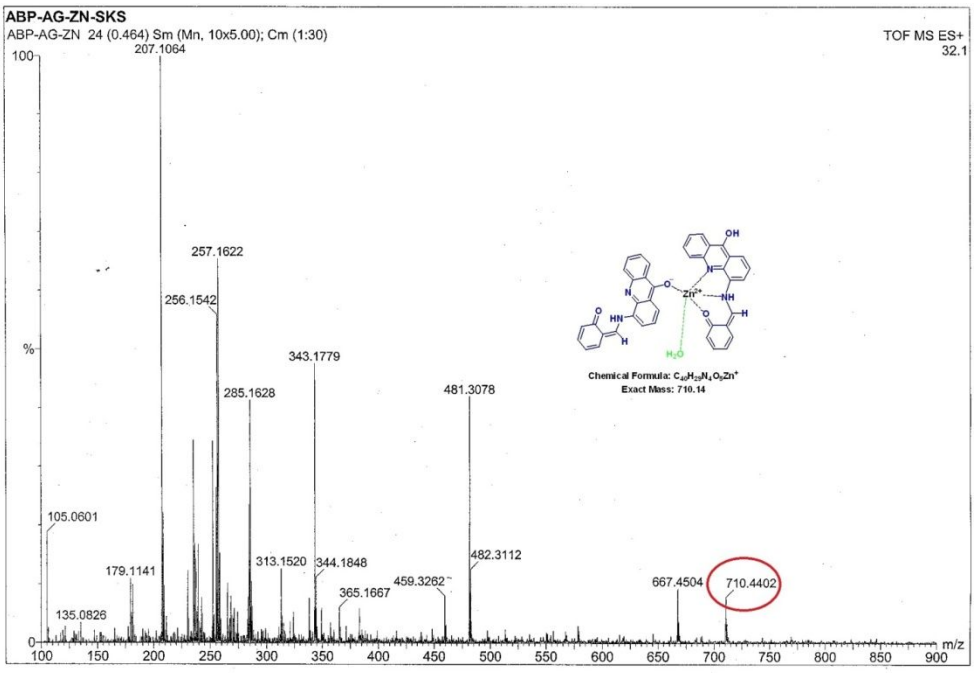

Figure S35 TOF MS spectrum of isolated **AAS**-Zn^{2+} complex in methanol.

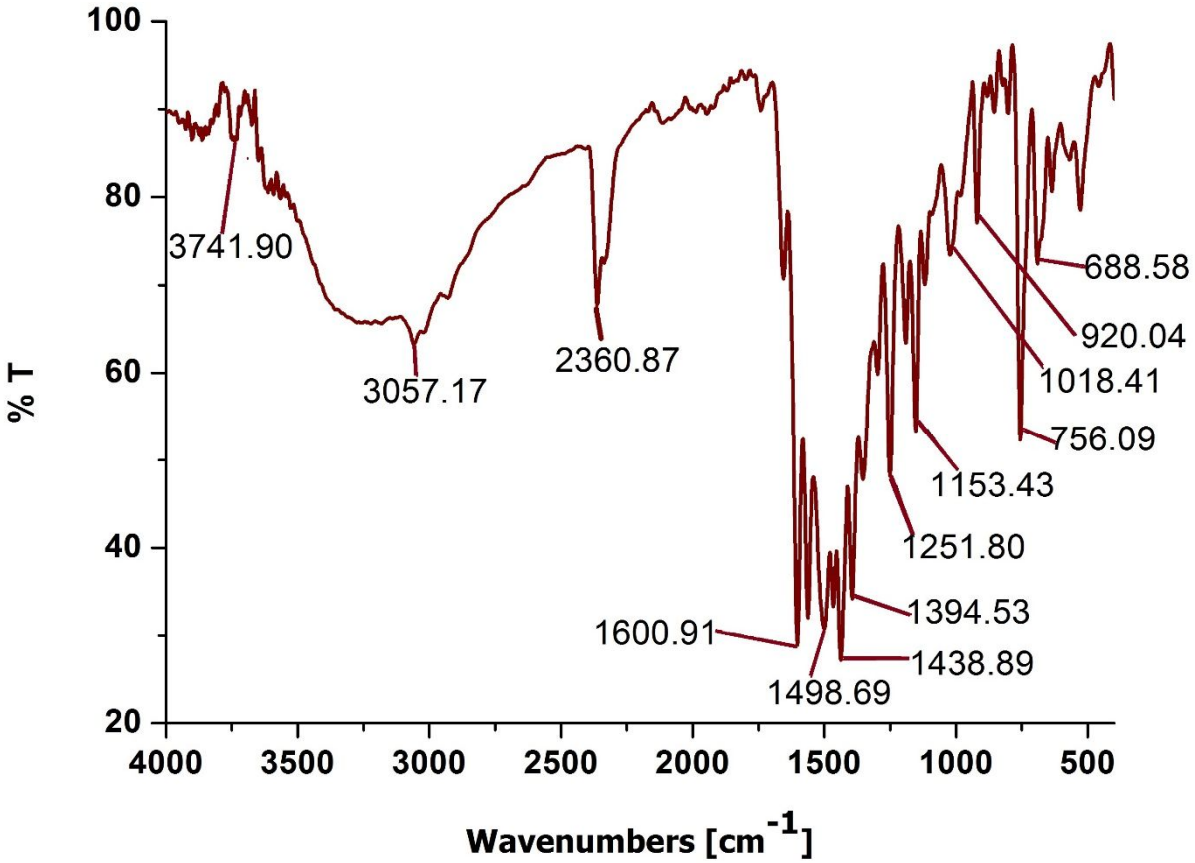

Figure S36 ATIR spectra of **AAS-Zn^{2+}** complex.

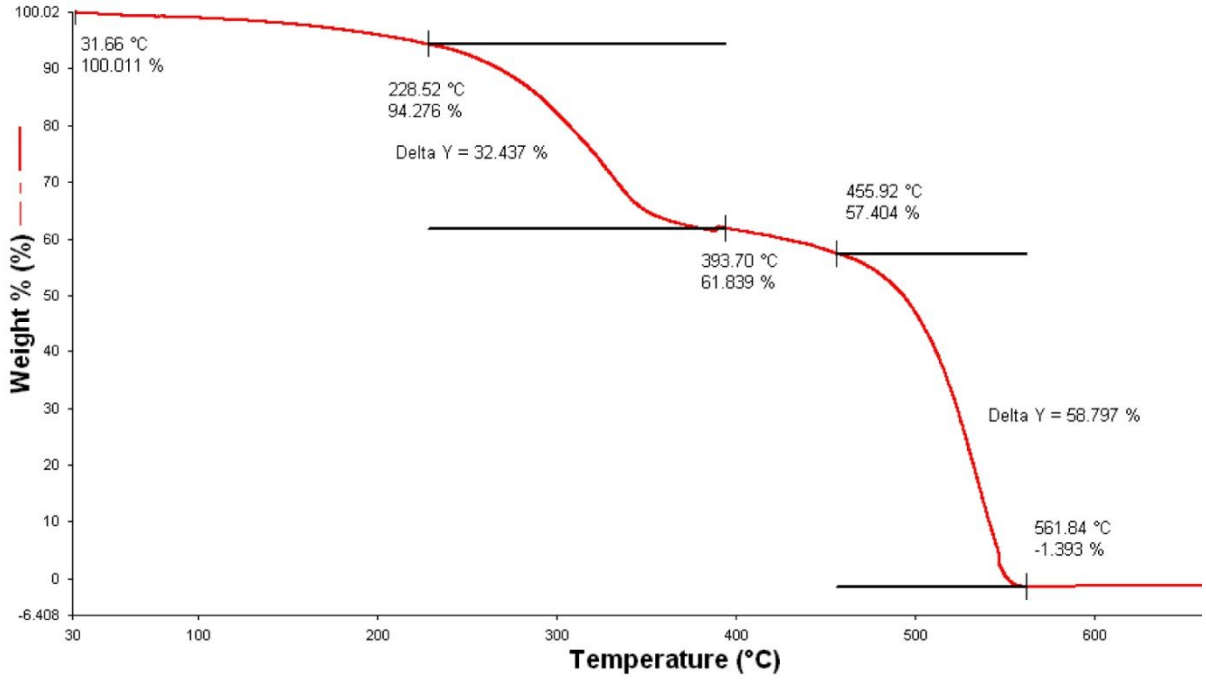

Figure S37 TGA of **AAS.**

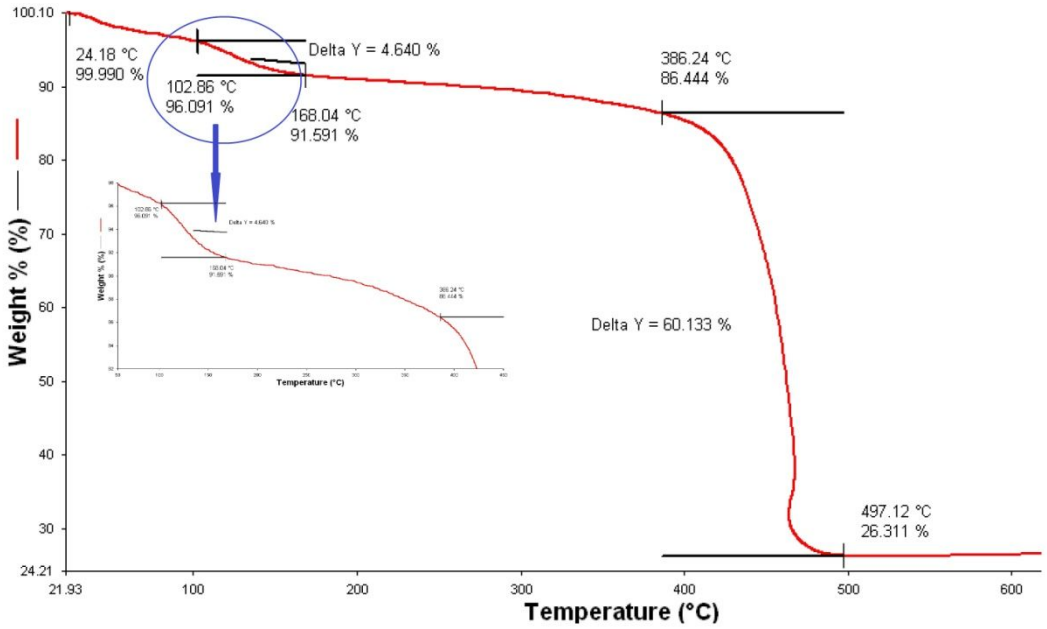

Figure S38 TGA of red coloured **AAS-Zn^{2+}** complex.

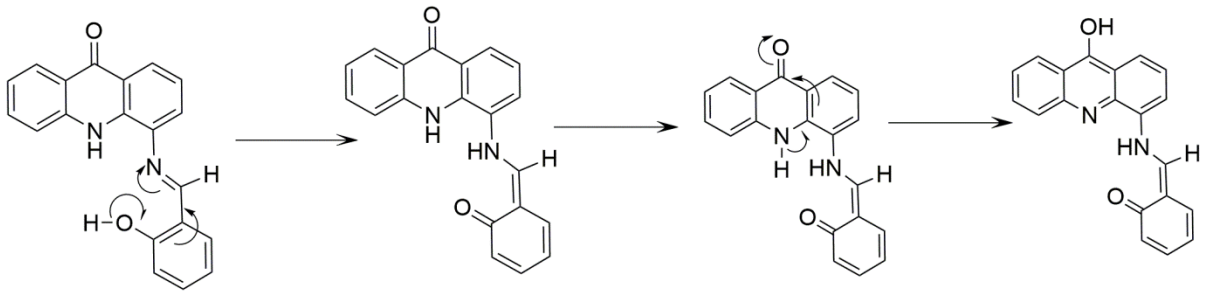

Figure S39 Probable mechanism of selective sensing of Zn^{2+} by **AAS**.

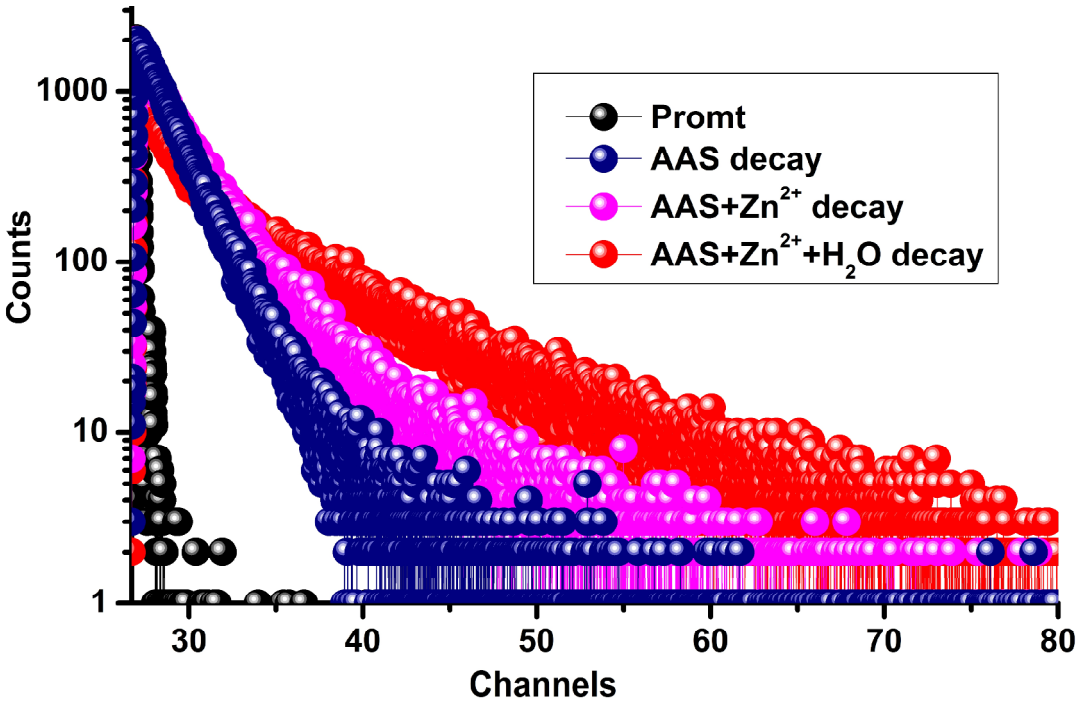

Figure S40 Fluorescence lifetime decay of **AAS**, **AAS+Zn^{2+}** and **AAS+Zn^{2+}+H_2O** at emission wavelength of 560 nm.

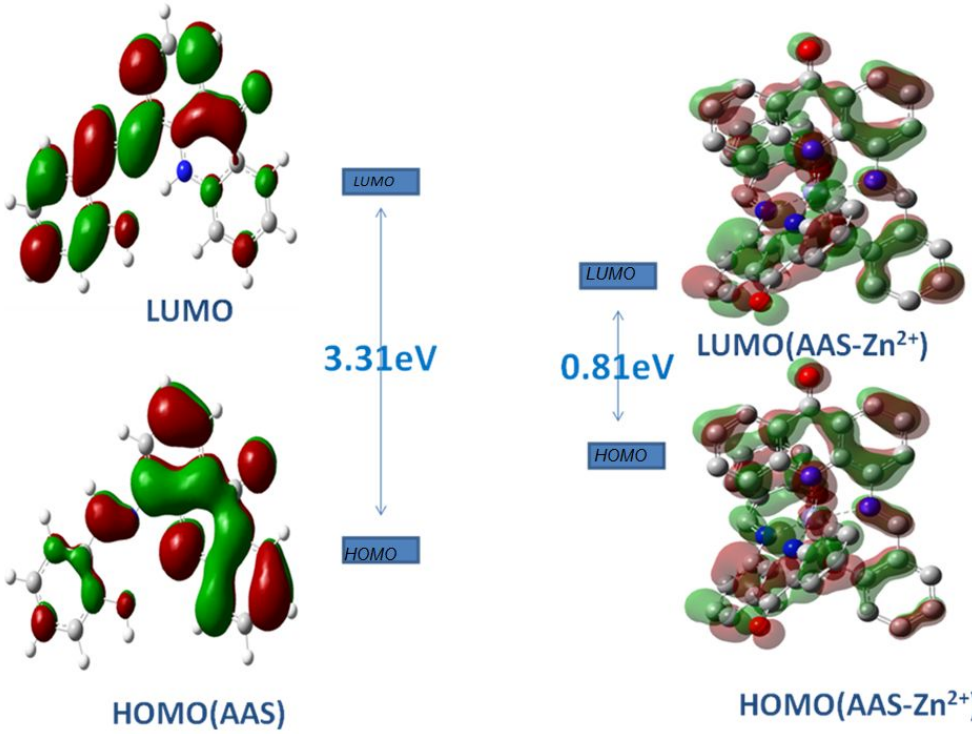

Figure S41 HOMO-LUMO energy gaps in **AAS** and **AAS-Zn^{2+}** adduct.

In vitro cell imaging

Human breast cancer cell line MCF7 are grown in DMEM (Sigma, St. Louis, USA) supplemented with 10% foetal bovine serum (Sigma, St. Louis, USA), 2 mM glutamine, 100 U/mL penicillin-streptomycin solution (Gibco, Invitrogen, USA) in the presence of 5% CO_2 at 37°C.For in vitro imaging studies, the cells are seeded in 6 well culture plates with a seeding density of 10^5 cells per well. After reaching 60%–70% confluence, the previous media was replaced with serum free media, supplemented with (50 µM) Zn^{2+} and incubated for 30min to facilitate metal ion uptake by cells. Then cells are washed three times with medium to remove extracellular Zn^2. Then 10 μM of **AAS** was added and incubated further for another 2 h. The cells are then observed under an inverted microscope (Dewinter, Italy) at different magnifications to examine any adverse effect on cellular morphology using blue filter. Images are taken through an attached CCD camera with the help of BioWizard 4.2 software.

Human cervical cancer HeLa cells were cultured in Dulbecco's modified eagle medium (DMEM) supplemented with 10% fetal bovine serum (FBS) and 1% penicillin/streptomycin at 37°C and 5% CO_2. For *in vitro* imaging studies, the cells are seeded in 6-well tissue culture plates with a seeding density of 10^5 cells per well. After reaching 60%–70% confluence, the previous DMEM medium was replaced with serum free DMEM medium, supplemented with 50 µM Zn^{2+} and incubated for 1h to facilitate metal ion uptake by cells. Then cells were washed three times with PBS buffer to remove extracellular Zn^{2+}. Then **AAS** (10 µM) was added into the medium and then further incubated for 1h. After washing with PBS buffer, images of live cells were taken by Olympus IX81 microscope.

Differential interference contrast (DIC) and fluorescence images of live cells were obtained by Olympus IX81 microscope using image-pro plus version 7.0 software.

In another experimental set up, human cervical cancer HeLa cells were cultured in Dulbecco's modified eagle medium (DMEM) supplemented with 10% fetal bovine serum (FBS) and 1% penicillin/streptomycin at 37°C and 5% CO_2. For *in vitro* imaging studies, the cells are seeded in 6-well tissue culture plates with a seeding density of 10^5 cells per well. After reaching 60%–70% confluence, the previous DMEM medium was replaced with serum free DMEM medium. Then **AAS** (10 µM) was added into the medium and then further incubated for 1h. In a control experiment, of 10 µM of **TPEN** was added to the medium and incubated for 30 min prior to addition of **AAS.** After washing the medium twice, 50 µM Zn^{2+} was added to the medium and incubated for 1h to facilitate metal ion uptake by cells. Then cells were washed three times with PBS buffer to remove extracellular Zn^{2+} after washing with PBS buffer, images of live cells were taken by Olympus IX81 microscope.

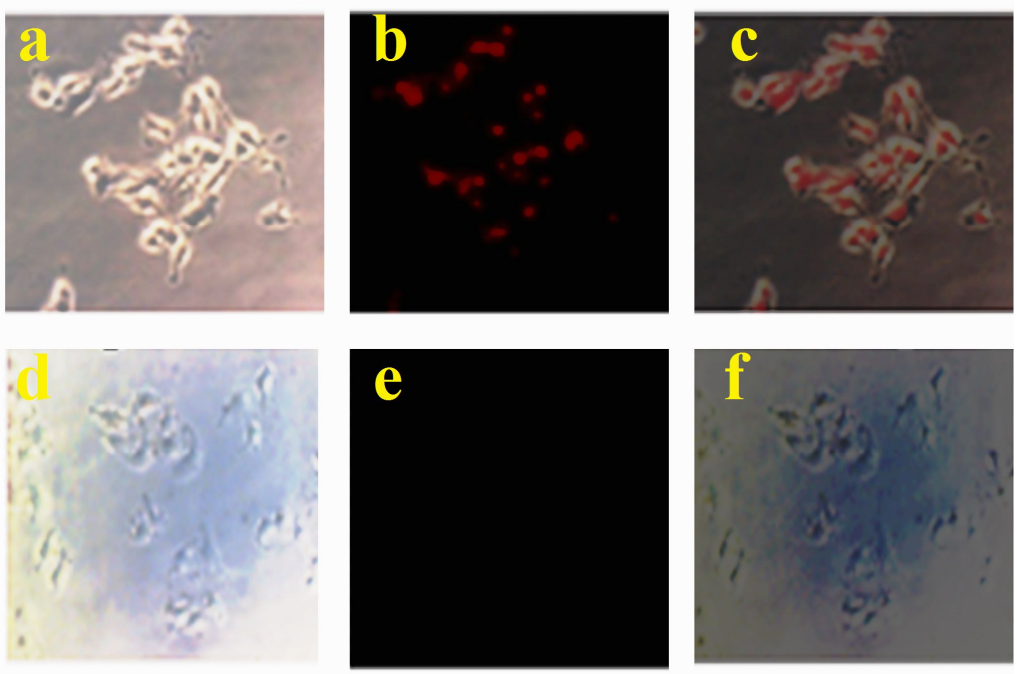

Figure S42 Fluorescence microscope images of HeLa cells after treatment with AAS (10 μM): (a) and (d) are bright field images in absence and presence of **TPEN (10 μM)** ; (b) and (e) are fluorescence images of cells after 30 min incubation with Zn^{2+} (50 μM) in absence and presence of TPEN; (c) and (f) are merged images.

Cytotoxicity assay

In vitro cytotoxicity was measured by using the methyl thiazolyl tetrazolium (MTT) assay in MCF7 cell lines. Cells were seeded into 96-well cell culture plate at 5×104 / well, 100% humidity cultured at 37 º C and 5 % CO_2 for 24 h, and then different concentrations of AAS (0, 10, 20, 50 and 100 μM) were added to the wells. The cells were then incubated for 30 min or 3h at 37 ºC under 5% CO_2. Subsequently, 10 μL MTT (5 mg/mL) was added to each well and incubated for an additional 3h at 37^{o}C under 5% CO_2. After addition of 10 % sodium dodecyl sulphate (SDS, 100 μL/well), the assay plate was allowed to stand at room temperature for 12 h. The following formula was used to calculate the inhibition of cell growth:

Cell viability (%) = (mean of Abs. value of treatment group / mean Abs. value of control) × 100%.

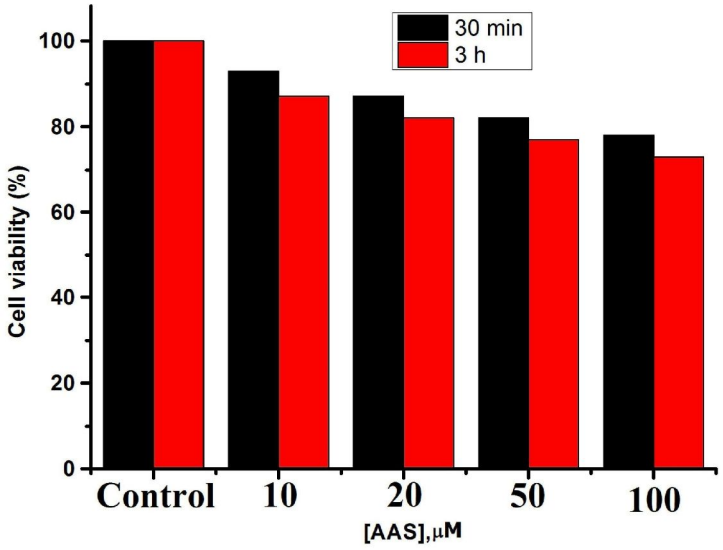

Figure S43 Cell viability values (%) *vs.* concentrations of AAS (10 to 100 μM) estimated by MTT assay test at 37 °C.